R-01-41

An empirical model of glacio-isostatic movements and shore-level displacement in Fennoscandia

Tore Påsse
Sveriges Geologiska Undersökning

August 2001

Svensk Kärnbränslehantering AB
Swedish Nuclear Fuel
and Waste Management Co
Box 5864
SE-102 40 Stockholm Sweden
Tel 08-459 84 00
+46 8 459 84 00
Fax 08-661 57 19
+46 8 661 57 19

ISSN 1402-3091
SKB Rapport R-01-41

An empirical model of glacio-isostatic movements and shore-level displacement in Fennoscandia

Tore Påsse
Sveriges Geologiska Undersökning

August 2001

Keywords: glacio-isostatic uplift, shore-level displacement, eustasy.

Abstract

Shore-level displacement in Fennoscandia is mainly due to two co-operative vertical movements, glacio-isostatic uplift and global eustatic sea level rise. The course of the glacio-isostatic uplift has been made discernible according to an investigation of the lake-tilting phenomenon (Påsse 1996a, 1998). This information made it possible to start an iteration process that has given mathematical expression for factors involved both within the isostatic movements and the eustatic rise.

There are two components involved in glacio-isostatic uplift. The main uplift, still in progress, acts slowly and is thus called the slow component. *Arctan* functions have proved to be suitable tools for describing the slow component. There are two main factors involved in the function used for calculation; A_s (m), the download factor (m) and B_s (y^{-1}), which is an inertia factor. A strong linear correlation between the inertia factor B_s and lithosphere thickness has been found in the model.

There was also a fast component involved in the crustal changes at the end of Late Weichselian and early Holocene. This component gave rise to fast subsidence followed by fast uplift during the final part of the deglaciation. Crustal subsidence is assumed to be due to reloading of the crust in the central parts of Fennoscandia during the Younger Dryas stadial. Normal distribution functions are used for calculating this component.

Glacio-isostatic uplift and thus a regressive shore-level displacement was extremely rapid around 10 300 years BP. This fast regression was contemporaneous and occurred in a similar way at the West Coasts of Norway and Sweden as well as in the Baltic. The "drainage" of the Baltic Ice Lake has been interpreted in the model as due to this fast regression.

The slow component is most probably due to viscous flow in the asthenosphere and the fast component is assumed to be due to its elasticity.

Sammanfattning

I området, som täcktes av den skandinaviska isen under den senaste istiden, utgör strandförskjutningen en funktion av två samverkande vertikala rörelser, glacial-isostatisk landhöjning och eustatisk havsytehöjning. Genom sjöstjälpningsmetoden har ett ungefärligt förlopp av landhöjningen kunnat fastställas (Påsse 1996a, 1998). Denna kunskap har gjort det möjligt att, i kombination med empirisk information från strandförskjutningskurvor och den nuvarande relativa landhöjningen, beskriva både landhöjningens och havsytans förändringar matematiskt.

Beskrivningen visar att landhöjningen styrs av två komponenter, en långsam och en snabb. Den långsamma komponenten utgör den största delen av den glacial-isostatiska landhöjningen och är en pågående rörelse. Denna komponent beskrivs med *arctan* funktioner. Det långsamma landhöjningsförloppet bestäms främst av två faktorer, A_s (m), nedtryckningsfaktorn och B_s (y^{-1}), som utgörs av en tröghetsfaktor. En stark linjär korrelation har konstaterats mellan tröghetsfaktorn B_s och litosfärens mäktighet.

I slutfasen av isavsmältningen, dvs i slutet av senweichsel och under tidig holocen, skedde en kortvarig snabb sänkning av jordskorpan, vilken omdelbart följdes av en lika snabb höjning. Dessa jordskorpsförändringar sammanfattas som den snabba komponenten och beskrivs med normalfördelningsfunktioner. Den kortvariga sänkningen antas bero på en tillväxt av inlandsisen och som följd av denna en förnyad nedpressning under Yngre Dryas stadialen. Landhöjningen och därmed strandförskjutningen var extremt snabb omkring 10 300 år BP. Efter den norska och den svenska västkusten, men också i forna Östersjön, skedde strandförskjutningen med liknande förlopp under denna tid. ”Baltiska Issjöns tappning” har tolkats som en snabb regression till följd av den snabba komponenten.

Contents

1 Method of the modelling

1.1 Objective

The objective is to find mathematical expressions that describe shore-level displacement and glacio-isostatic uplift in the area covered by Scandinavian ice during the Weichselian glaciation. As the mathematical expressions are based solely on empirical data, they can be used for evaluations of both geological and geophysical parameters involved in the glacio-isostatic process. The model is purely empirical while most other models are based on more or less well-supported assumptions about ice thickness, deglaciation rates and geophysical parameters.

The author, in SKB Technical Reports (1996b, 1997), presented two mathematical expressions of shore-level displacement in Fennoscandia. Påsse & Andersson (2000) transformed the last model into a GIS application. Earlier works was mainly based on shore-level data from the coastal areas. Utilising information about relative recent uplift from precision levellings extends this third part of the work. Using this information means that the empirical model also includes inland areas.

1.2 Method

Shore-level displacement (S m) in Fennoscandia is mainly due to two interactive vertical movements, glacio-isostatic uplift (U m) and global eustatic sea level rise (E m), Figure 1-1. Shore-level displacement is estimated by:

$$S = U - E \qquad \text{Equation 1-1}$$

If the eustatic rise of the sea level were known in detail it would have been possible to calculate the glacio-isostatic uplift directly from the shore-level curves. Fairbanks (1989) has published a eustatic curve, which is generally accepted and commonly used in shore-level modelling. As will be demonstrated later (Chapter 2.2) the reliability of this curve is insufficient and therefore cannot be used for accurate shore-level calculations.

Physical models of glacio-isostatic uplift have been presented in recent years by e.g. McConnel (1968), Cathles (1975), Peltier (1976, 1988, 1991), Clark et al. (1978), Nakada & Lambeck (1987, 1989), Fjeldskaar & Cathles (1991), Lambeck (1991), Nakiboglu & Lambeck (1991) and Lambeck et al. (1998). The formulae for the course of glacio-isostatic uplift, used in these models, are mainly derived from rheological parameters. However the authors have quite different opinions about these parameters.

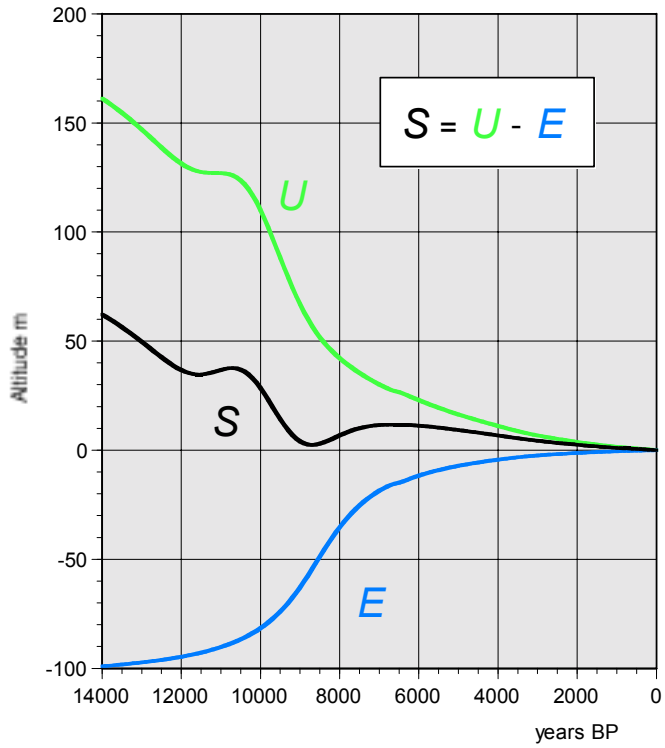

Figure 1-1. *Eustasy (E) and crustal uplift (U) determine shore- level displacement (S), by S = U - E.*

Påsse (1990a, 1996a, 1998) investigated glacio-isostatic uplift based on the lake-tilting method. Lake-tilting data show the difference in the course of crustal uplift between two sites, Figure 1-2. The point with empirical lake-tilting investigations is that the course of glacio-isostatic uplift can be expressed in mathematical terms without using rheological assumptions. By magnifying the function, which describes the lake-tilting, it has been possible to start an iteration process to create a mathematical expression of the shore-level displacement.

The main input data, besides the lake-tilting information, are shore-level curves from the area covered by Scandinavian ice during the Late Weichselian. The shore level curves are compared to the curves derived from the mathematical expressions. Information concerning present relative uplift (mm/y), recorded by precision levelling and tide gauge data, has also been used. In Finland records are presented by Kääriäinen (1963, 1966), Suutarinen (1983) and Kakkuri (1987), in Sweden by RAK (1971, 1974), in Denmark by Simonsen (1969) and Andersen et al. (1974), in Norway by Bakkelid (1979). The map of the present relative uplift presented by Kakkuri (1987) is shown in Figure 1-3. Ekman (1996) has compiled information of the present rate of crustal movements in Fennoscandia mainly from the sources mentioned above, Figure 1-4.

Recent relative uplift recorded by tide gauge data includes eustatic changes. A eustatic rise in the order of 1 mm/year has been reported by several authors including Lizitzen (1974), Mörner (1977, 1980a) and Ekman (1986). Compilations by Emery & Aubrey (1991) and Nakiboglu & Lambeck (1991) indicate a present eustatic rise in the order of 1.2 mm/year. Lambeck et al. (1998) estimates the present rise to 1.05 mm/year.

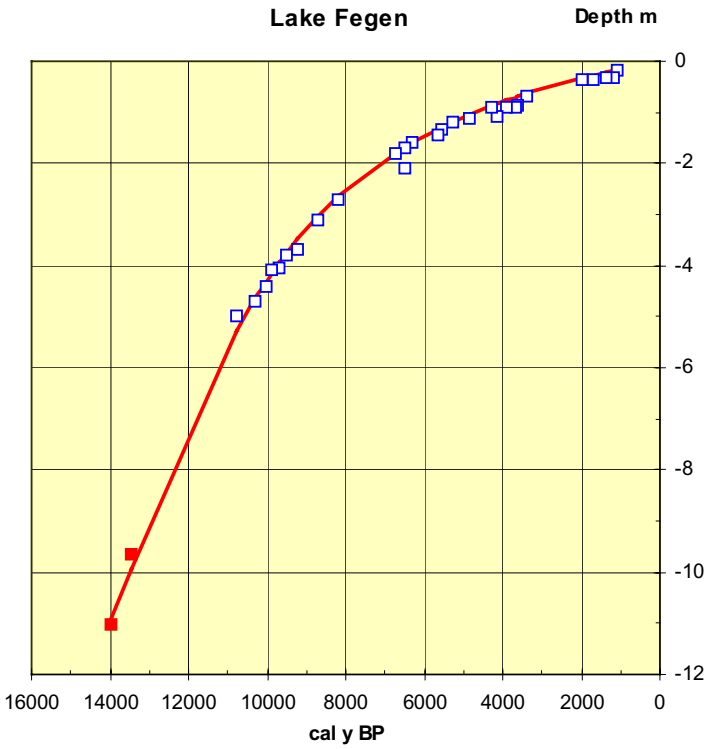

Figure 1-2. *Radiocarbon dates for ancient lake levels in lake Fegen (Påsse 1990a, 1996a). The two lowermost points, denoted by red squares, are derived from the gradient of shorelines formed during formation of the Göteborg moraine and the Berghem moraine. The curve shows difference in land uplift between the outlet and the southern part of the lake expressed by an arctan function.*

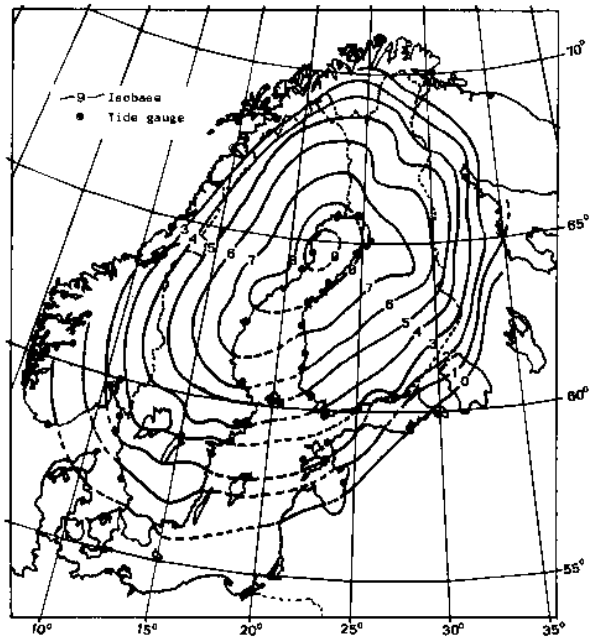

Figure 1-3. *Recent relative uplift (mm/y) according to Kakkuri (1987).*

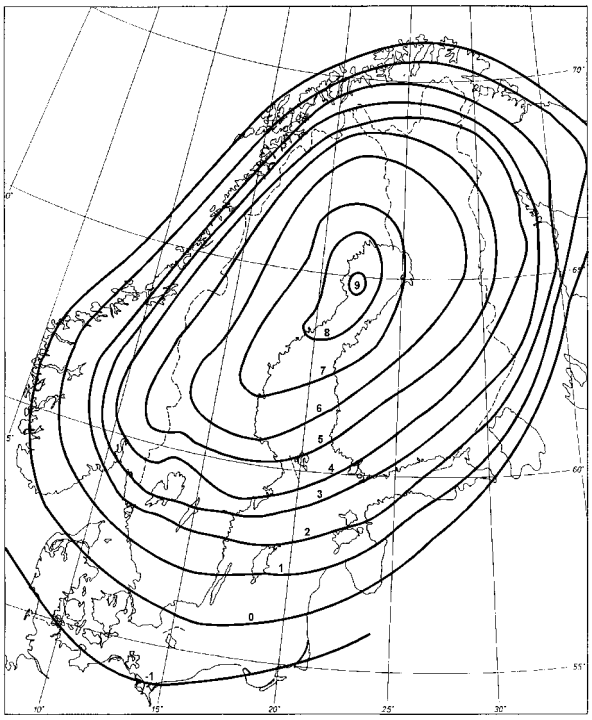

Figure 1-4. *Recent relative uplift (mm/y) recorded by precision levelling and tide gauge data. The map is redrawn from Ekman (1996).*

The present knowledge about ice recession of the Scandinavian ice during the late Weichselian is summarised in Andersen et al. (1998). The Scandinavian ice reached its maximum about 20 000 years BP, Figure 1-5. During the first 5 000 years of the deglaciation the ice recession rate was very low. Between 15 000 and c. 11 000 years BP the ice recession rate increased but was still relatively low. This is due to the climatic conditions, which can be designated as arctic or subarctic during this time. Between 11 000 and c. 10 300 years BP, i.e. during the Younger Dryas stadial, there was a severe climatic deterioration when the inland ice once more grew and the ice border advanced again. This phase gave rise to the formation of the Younger Dryas terminal moraines. At 10 300 years BP there was a sudden rise in temperature and less than 2 000 years later the whole Fennoscandia was ice free. In summary the ice recession can be divided into three intervals;

- 20 000–11 000 years BP comprises a slow deglaciation in the peripheral parts.
- 11 000–10 300 years BP comprises a regeneration of the inland ice.
- 10 300–8 500 years BP comprises a very rapid deglaciation and final retreat of the ice in central Fennoscandia.

According to a shore-level curve from Andöja (Vorren et al. 1988), glacio-isostatic uplift started around 16 000 years BP.

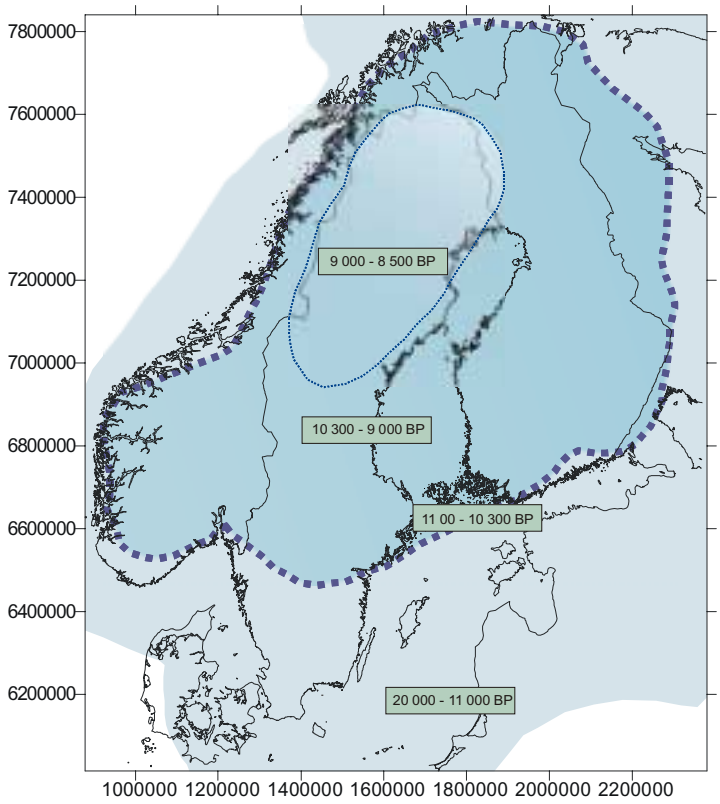

Figure 1-5. Ice recession in Fennoscandia can be divided into three intervals. Between c. 20 000 and 11 000 years BP there was a slow ice recession in the peripheral parts. Between 11 000 and 10 300 years BP there was a regeneration of the inland ice and the Younger Dryas terminal moraines were formed. The period from 10 300 to 8 500 years BP comprises a very rapid deglaciation and a final retreat of the inland ice in central Fennoscandia.

1.3 Calibration of ^{14}C-values

Most shore-level curves refer to conventional ^{14}C-dates. However, for calculating the glacio-isostatic uplift it is necessary to use calendar years. A mathematical expression for converting conventional ^{14}C-dates to calendar dates is derived in Påsse (1996b). The formula used in the modelling for converting dates is written as:

$$t = 59.6 - 206.9 \cdot \arctan\left[\frac{(4000 - 1.095 \cdot t_{con})}{800}\right] +$$

$$63.66 \cdot \arctan\left[\frac{(7200 - 1{,}095 \cdot t_{con})}{100}\right] +$$

$$95.5 \cdot \arctan\left[\frac{(750 - 1.095 \cdot t_{con})}{200}\right] + 1.095 \cdot t_{con} \qquad \text{Equation 1-2}$$

where t is the calibrated date, while t_{con} is the conventional radiocarbon date. When calendar years are used, this is pointed out by writing cal years BP, while conventional ^{14}C-years is denoted as years BP.

2 Formulae used in the modelling

2.1 General

Iterative calculations provide a base for the modelling. Crustal changes are described using simple expressions and the formulae used should be seen as rough tools for calculations and as support for interpretation. At each site crustal change is described by one arctan function and one normal distribution function. One of the advantages with these functions is that they can be used to simplify the calculations and to show regularities or irregularities within the crustal processes.

In both functions used for calculation there are three factors, which are named *A*, *B*, and *T*. *A* designates the amounts of crustal change. *B* is explained as an inertia factor, which describes the declining or inclining velocity of the crustal changes. *T* designates the time for the maximal uplift rate in the arctan function and the time for the maximal (or minimal) amount of uplift (or subsidence) in the normal distribution function. The eustatic rise is calculated in a similar way by using an arctan function, where the three factors correspond to the amount of eustatic rise, the declining or inclining velocity of the eustasy and the time of the maximal rise.

The choice of functions implies that 6 factors had to be estimated at each locality. As the eustatic rise was also included in the calculations 9 factors had to be included in the iteration process. By holding some of the factors constant and slowly approaching likely combinations for the remaining factors, the iteration process was made possible. In this way regularities and irregularities were found in the shore-level process which limited the number of the final factors to five. One fact that simplifies the iteration is that the factors show regional regularities. The values of factors are later presented in isoline maps, which can be said to be the framework of the empirical model.

2.2 The eustasy

2.2.1 Sea level changes

Ever since Godwin et al. (1958), Fairbridge (1961), Jelgersma (1961) and Shepard (1963) presented eustatic curves of the global sea level rise there have been several subsequent curves, showing the same trend but differing in detail. A eustatic curve from Barbados, published by Fairbanks (1989) based on radiocarbon dated corals, is the most generally accepted curve today. This curve goes back to 18 000 years BP and the global sea level were measured to about –120 m.

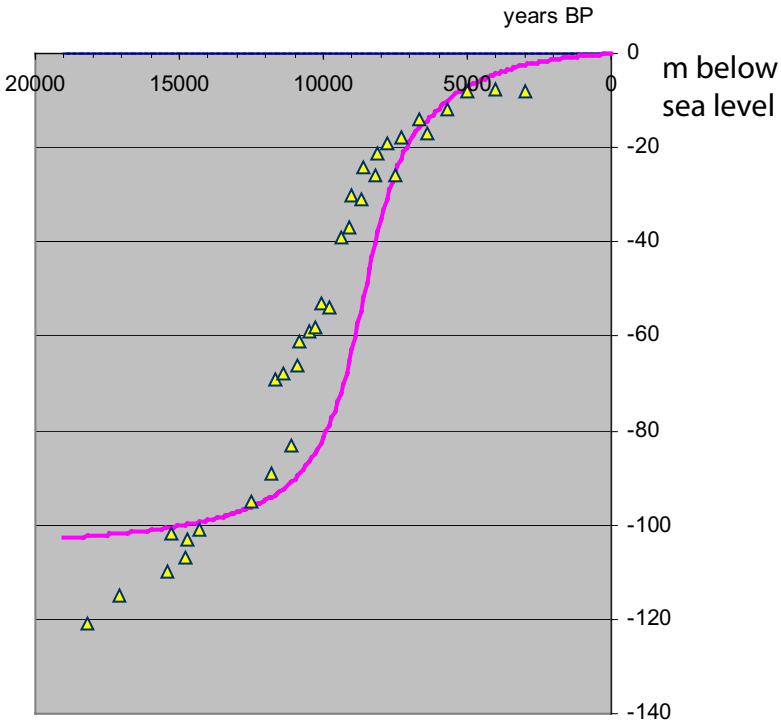

Figure 2-1. *Eustatic development. The yellow triangles show dates of corals from Fairbanks (1989). The red curve is the eustatic curve received as a result from the calculations.*

By calculating the difference between hypothetical uplift curves and empirical shore-level curves it has been possible, by iteration, to estimate a function for the eustasy. The main course of the eustatic rise may be expressed as:

$$E = \frac{2}{\pi} \cdot 56 \cdot \left[\arctan\left(\frac{9500}{1350}\right) - \arctan\left(\frac{9500 - t}{1350}\right) \right] \qquad \text{Equation 2-1}$$

t in Equation 2-1, is in calendar years. The figure 9500 in this formula means the time for the maximal rate of eustatic rise in calendar years (about 8 575 years BP) and the figure 56 designates half of the total eustatic rise (in m). This figure shows that eustatic rise since the glacial maximum is estimated to 112 m and differs from the value reported by Fairbanks (1989) by 8 meters. However, information concerning the eustasy has only been calculated back to 14 000 years BP in the modelling. A comparison between the coral dates, forming the basis of Fairbanks' curve, and the calculated curve is shown in Figure 2-1.

Equation 2-1 for the eustasy only takes the main rise into consideration. In areas where the tidal effect is very low and raised shore-levels exist, it is obvious that sea level not only rose continuously during Holocene but also changed in an oscillatory way (cf. Påsse 1983). The size and periodicity of these oscillations are not well established but it is difficult to leave such information unnoticed in this context. A sinusoidal function may be added to the main eustatic formula in order to attain more detailed information

regarding transgression and regression phases. The sinusoidal function is preliminary given a periodicity of about 475 years (Påsse 1983) and amplitude of 0.5 m. The cyclic function can be written as:

$$C = 0.5 \cdot \sin\left[(t - 100) \cdot 0.013\right] - 0.48 \qquad \text{Equation 2-2}$$

It is hard to estimate a true global eustatic curve, as there are several factors that locally affect sea level rise. Among these factors are hydro-isostasy and gravitation. The eustatic curve, which is obtained from the modelling, may thus include components from other processes than the true eustasy. This is also valid for Fairbanks' (1989) curve.

2.2.2 Water level changes in the Baltic

The accepted model of the development of the Baltic is that there have been two lake phases, the Baltic Ice Lake and the Ancylus Lake. The model presented in this report shows that the water level of the Baltic was only higher than the global sea during the Ancylus Lake phase. The difference between the water level in the Ancylus Lake and the global sea has been considered in the calculations. A more detailed analysis of the development in the Baltic basin is presented in Chapter 5.

2.3 Uplift formulae

There are two components involved in glacio-isostatic uplift. The main uplift, still in progress, acts slowly. This component is calculated by arctan functions and is called the slow component. During the deglaciation phase there was another component involved in the crustal changes, which gave rise to fast crustal changes of short duration. This component is calculated by a normal distribution function and is called the fast component. The nature of the two components will be further discussed in Chapter 4.

2.3.1 The slow component

According to Andrews (1970) glacio-isostatic movement starts slowly, reaches a maximal rate and after that follows a declining course. Different S-shaped functions have been tested for describing glacio-isostatic uplift from lake-tilting information (Påsse 1996a) and shore-level data (Påsse 1996b). Arctan functions turned out to be the most suitable way of describing glacio-isostatic uplift following the slow component. An arctan function can roughly be regarded as a cumulative normal distribution function.

The arctan functions can be divided into two symmetrical parts, one inclining and the other declining. To say that the initial inclining phase of uplift is symmetrical to the declining phase is an overstatement as there is too little information accessible for testing the inclining phase. The lack of data is due to the fact that the main part of

uplift, during the inclining phase, occurred beneath a cover of ice. Only the declining phase of the function can be tested for its validity of describing glacio-isostatic uplift. Land uplift following unloading of ice (U_s in m) can then be described with the function:

$$U_s = A_s - \frac{2 \cdot A_s}{\pi} \cdot \arctan\left(\frac{T_s - t}{B_s}\right) - \left[A_s - \frac{2 \cdot A_s}{\pi} \cdot \arctan\left(\frac{T_s}{B_s}\right)\right] \qquad \text{Equation 2-3}$$

simplified as:

$$U_s = \frac{2}{\pi} \cdot A_s \cdot \left[\arctan\left(\frac{T_s}{B_s}\right) - \arctan\left(\frac{T_s - t}{B_s}\right)\right] \qquad \text{Equation 2-4}$$

where A_s is a down load factor (m), T_s (years) is the time for the maximal uplift rate, i.e. the symmetry point of the arctan function, t (year) is the variable time and B_s (y^{-1}) is an inertia factor. In the calculations T_s and t are counted in calendar years according to Equation 1-2. However, within all graphs the dates are reported in conventional ^{14}C-years, as these dates are more familiar to most geologists. Graphs of slow glacio-isostatic uplift calculated by different values of A_s and B_s are shown in Figure 2-2.

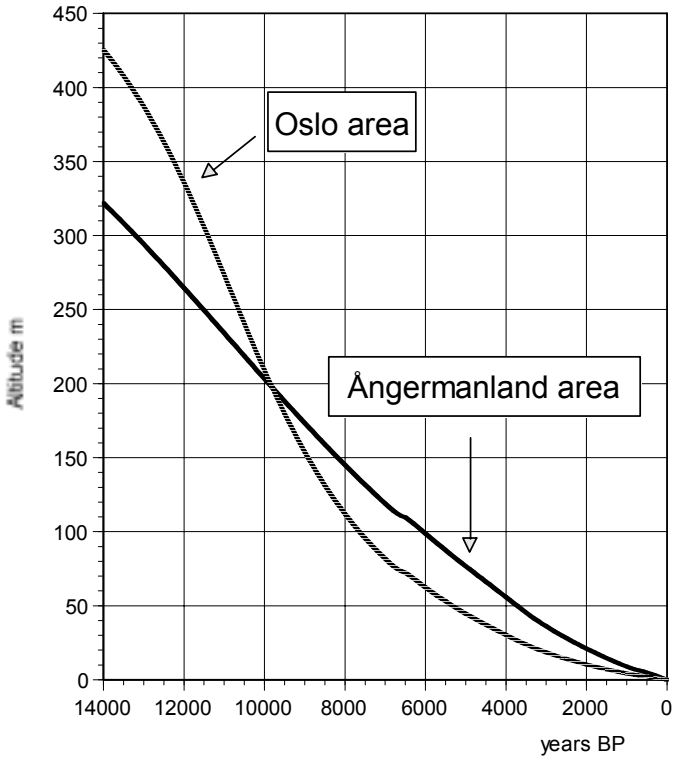

Figure 2-2. *Graphs of slow glacio-isostatic uplift calculated at Oslo area and Ångermanland area. The uplift in the Oslo area is calculated with A_s = 320 m and B_s = 3 400. The uplift in the Ångermanland area is calculated with A_s = 380 m and B_s = 8 800. Notice that total uplift in the Oslo area up to now is higher than in the Ångermanland area, despite a lower value of A_s. This is explained by the inertia effect, which predicts a larger remaining recovery in the Ångermanland area, while most of the recovery already has occurred in the Oslo area.*

In the arctan formula, A_s defines half the amount to which the function reaches. The formula used is only valid from about 16 000 years BP i.e. when the deglaciation accelerated. In order to estimate the "total" uplift the variable A_s should be multiplied by 1.5 or 1.6.

The factors A_s and B_s differ regionally while T_s seems to be regionally constant and is estimated to 12 000 calendar years BP i.e. 10 850 years BP counted in the conventional radiocarbon chronology. The formula for the slow uplift can thus be written as:

$$U_s = \frac{2}{\pi} \cdot A_s \cdot \left[\arctan\left(\frac{12000}{B_s} \right) - \arctan\left(\frac{12000 - t}{B_s} \right) \right] \qquad \text{Equation 2-5}$$

2.3.2 The fast component

Shore-level curves from Norway and from the northern parts of the Swedish West Coast, i.e. areas outside but close to the Younger Dryas ice border, show crustal subsidence during Alleröd and Younger Dryas (about 12 000–10 300 years BP). This subsidence was restored by fast uplift. Fast uplift lasted at some sites about 1000–2000 years but was usually of much shorter duration. Fast uplift during early Holocene is especially significant in central Fennoscandia and recorded in all shore-level curves from this area.

In the present model the fast component is calculated by a normal distribution function, where the first half of the function describes subsidence and the second half uplift.

A general formula for the fast component is:

$$U_f = A_f \cdot e^{-0.5 \cdot \left(\frac{t - T_f}{B_f} \right)^2} \qquad \text{Equation 2-6}$$

where U_f is the crustal change (m), A_f is the total subsidence/uplift (m), B_f is the inertia factor (y^{-1}), t is the variable time (year) and T_f is the time for the maximal subsidence/uplift, i.e. the symmetry point of the function. T_f has small regional differences and varies between 11 800 to 11 200 cal years BP (10 700 to 10 100 y BP). These regional differences are reported in Table 3-1 but are also shown later in Figure 3-15.

The course of the crustal movements caused by the fast component is shown in Figure 2-3. The total glacio-isostatic uplift can be calculated by combining the effects of the slow and fast components, Figure 2-4.

From a mathematical viewpoint the fast component can be regarded a separate factor. The fast component is described by a normal distribution function, which predicts subsidence followed the same amount of uplift. However, in areas where slow uplift rate is high this "subsidence" is reflected as retardation in uplift.

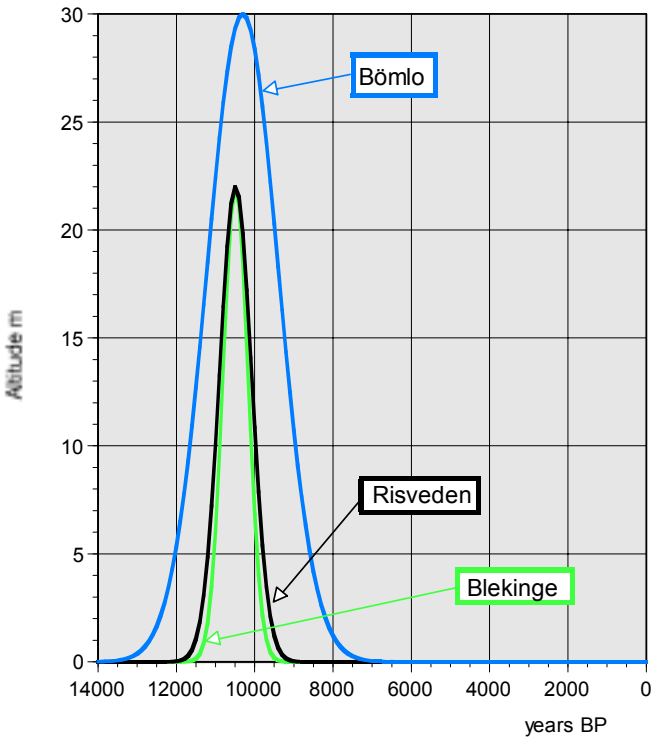

Figure 2-3. *The course of the crustal movements caused by the fast component at Bömlo, Blekinge and Risveden. The values used for the calculations are reported in Table 3-1. Notice that the fast components are more or less equal at Blekinge and at Risveden.*

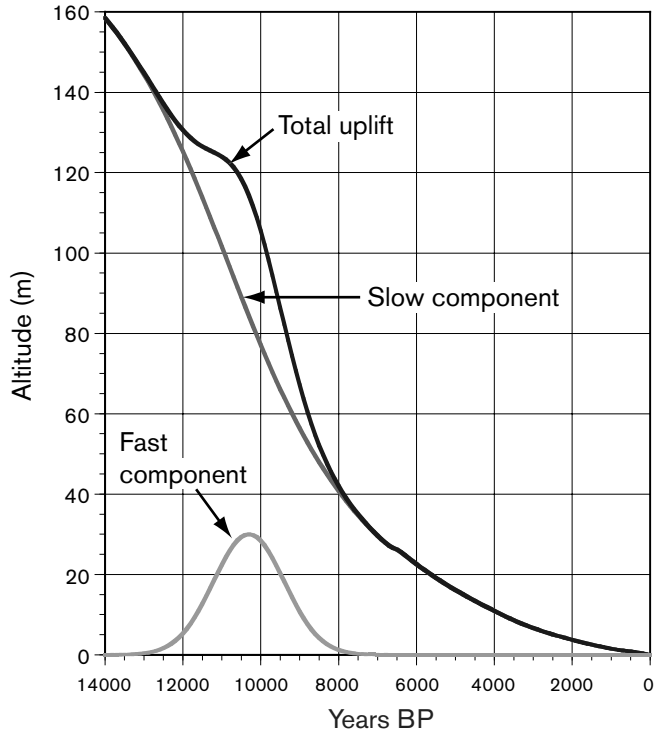

Figure 2-4. *Crustal movements at Bömlo area. The sum of the slow component and the fast component makes up the total or actual uplift.*

3 Results of the modelling

3.1 Shore-level curves

72 shore-level curves from the area covered by Scandinavian ice during the Late Weichselian were used as input data. These shore-level curves were compared to curves deduced from the formulas presented in Chapter 2. Each curve used in the analysis is designated with a site number. The references of the shore-level curves are presented in Table 3-1. The values of A_s, B_s, A_f, B_f and T_f that generate the best correlation between original and calculated shore-level curves are reported in the same table. T_s is always set to 12 000 years BP. Sites, which are illustrated by shore-level curves, are marked with an asterisk in Table 3-1. Geographical positions of the sites are shown in Figure 3-1. Some examples of the comparisons between original and calculated shore-level curves are shown in Figure 3-2 to Figure 3-5 but also in Figure 5-1. The theoretical curves are calculated without using the oscillation formula for the eustatic component, Equation 2-2, but examples of calculations, where the oscillation function is included, are given in Figure 3-3. Some shore-level curves are complemented or extended by new data from nearby sites. The shore-level curve from Östfold (Danielsen 1970) has been divided in two parts, as the investigation area is too vast. Recent absolute uplift was calculated at each site. These calculations confirm earlier estimations of an ongoing eustatic rise of about 1.1 mm/y.

Table 3-1. Number, names and references of the sites used in the calculations. Sites, which are illustrated by shore level curves, are marked with an asterisk.

Nr	Site	A_s	B_s	A_f	T_f	B_f	References
1	Varanger	170	3400	20	11400	800	Donner 1980
2	Andöja*	91	3200	20	11200	1100	Vorren et al. 1988
3	Tromsö	125	3300	24	11200	900	Hald & Vorren 1983
4	Lofoten	105	3200	18	11200	1000	Möller 1984, Vorren & Moe 1986
5	Näröy	260	3500	55	11200	800	Ramfjord 1982
6	Verdalsöra	295	3600	55	11200	750	Sveian & Olsen 1984
7	Frosta	290	3600	50	11200	750	Kjemperud 1986
8	Bjugn*	210	3400	50	11200	850	Kjemperud 1986
9	Hitra	180	3400	34	11200	850	Kjemperud 1986
10	Tjeldbergodden	178	3400	36	11200	850	Solem & Solem 1997
11	Fröja	152	3300	23	11000	800	Kjemperud 1986
12	Leinöy*	99	3150	18	11400	800	Svendsen & Mangerud 1990
13	Fonnes*	118	3300	35	11400	1000	Kaland 1984
14	Sotra	120	3300	34	11400	900	Krzywinski & Stabell 1984, Kaland et al. 1984
15	Bömlo	118	3300	30	11400	1000	Kaland 1984
16	Yrkje	118	3300	40	11400	800	Anundsen 1985
17	Hardanger	215	3400	55	11400	800	Helle et al. 1997
18	Jären*	93	3200	38	11400	1000	Thomsen 1981, Bird & Klemsdal 1986
19	Kragerö*	215	3300	70	11400	800	Stabell 1980
20	Porsgrunn	235	3400	75	11400	800	Stabell 1980
21	Vestfold	245	3400	60	11400	800	Henningsmoen 1979
22	Oslo	320	3400	90	11400	800	Hafsten 1983
23	Östfold	260	3400	55	11400	700	Danielsen 1970
24	Östfold N	285	3400	65	11400	800	Danielsen 1970
25	Ski*	310	3400	80	11400	900	Sörensen 1979
26	Jylland	120	3100	7	11600	300	Rickardt 1996
27	Vedbäck*	98	2500	5	11600	250	Christensen 1993
28	Söborg SÖ	96	2400	5	11600	250	Mörner 1976
29	St Bält	65	2300	5	11600	250	Christensen 1993, Bennike & Jensen 1995, Jensen et al. 1999
30	Kroppefjäll	255	3500	25	11500	500	Björck & Digerfeldt 1991
31	Hunneberg	237	3650	23	11600	450	Björck & Digerfeldt 1982
32	Central Bohuslän	225	3400	22	11600	450	Miller & Robertsson 1988
33	Ljungskile	205	3450	20	11600	450	Persson 1973
34	Risveden*	198	3450	22	11600	450	Svedhage 1985
35	Göteborg	162	3400	10	11600	300	Påsse 1983
36	Sandsjöbacka*	155	3400	8	11600	300	Påsse 1987
37	Fjärås	148	3350	6	11600	300	Påsse 1986
38	Varberg	132	3300	5	11600	300	Påsse 1990b, Berglund 1995
39	Falkenberg*	122	3250	5	11600	300	Påsse 1988
40	Halmstad	116	2850	5	11600	300	Caldenius et al. 1949, Caldenius et al. 1966, Berglund 1995
41	Bjäre Peninsula*	111	2800	5	11600	300	Mörner 1980
42	Barsebäck	97	2300	5	11600	250	Digerfeldt 1975, Persson 1962, Ringberg 1989
43	Blekinge*	122	2400	22	11600	350	Björck 1979, Liljegren 1982
44	Öland	125	2450	22	11600	375	Gembert 1987
45	Oskarshamn*	163	2600	24	11600	400	Svensson 1989
46	Gotland*	169	2600	17	11600	300	Svensson 1989
47	NE Småland	195	4000	40	11600	400	Robertsson 1997
48	Rejmyra*	230	4700	75	11600	600	Persson 1979
49	Stockholm area*	235	6200	85	11600	650	Åse 1970, Miller & Robertsson 1982, Brunnberg et al.1985, Risberg 1991, Hedenström & Risberg 1999

Nr	Site	A_s	B_s	A_f	T_f	B_f	References
50	Eskilstuna	255	6200	90	11500	700	Robertsson 1991
51	Närke	255	4700	70	11500	600	Hedenström & Risberg 1999
52	Gästrikland	320	7500	105	11400	1000	Asklund 1935
53	Hälsingland	355	7900	140	11400	1600	Lundqvist 1962
54	Ångermanland*	380	8800	160	11400	1900	Cato 1992
55	S. Västerbotten	380	9000	160	11400	1900	Renberg & Segerström 1981
56	Rovaniemi	330	9000	145	11400	1300	Saarnisto 1981
57	Lauhanwuori*	320	8800	145	11500	1250	Salomaa 1982, Salomaa & Matiskainen 1983
58	Olkiluoto*	258	7600	90	11600	850	Eronen et al. 1995
59	Åland	258	7200	90	11600	850	Glückert 1978
60	Turku	230	6800	85	11600	800	Glückert 1976, Salonen et al. 1984
61	Karjalohka	198	5700	75	11600	750	Glückert & Ristaniemi 1982
62	Tammisaari*	190	5500	75	11600	675	Eronen et al. 1995
63	Lohja	190	5600	75	11600	750	Glückert & Ristaniemi 1982
64	Espo	180	4800	72	11600	675	Hyvärinen 1980, 1984, Glückert & Ristaniemi 1982, Eronen & Haila 1982
65	Porvoo*	168	4400	70	11600	750	Eronen 1983
66	Hangassuo	165	4300	60	11600	750	Eronen 1976
67	St. Petersburg*	95	3200	25	11500	400	Dolukhanov 1979
68	Narva*	115	2700	38	11800	250	Kessel & Raukas 1979
69	Tallin*	165	3200	40	11800	250	Kessel & Raukas 1979
70	Köpu	165	3600	55	11800	350	Kessel & Raukas 1979
71	S Lithuania	105	2200	18	11600	200	Kabailiené 1997
72	W Baltic*	45	2200	0	11600	150	Winn et al. 1986, Klug 1980
73	Dalnie Zelentsy	138	3100	22	11500	950	Snyder et al. 1996

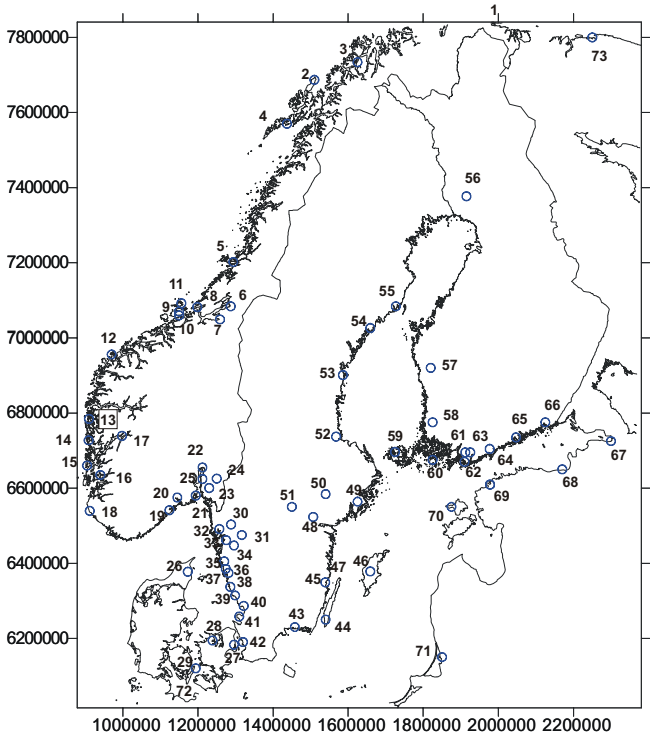

Figure 3-1. *Position of shore-level curves used in the modelling. Numbers refer to Table 3-1, where names of the sites and references are listed.*

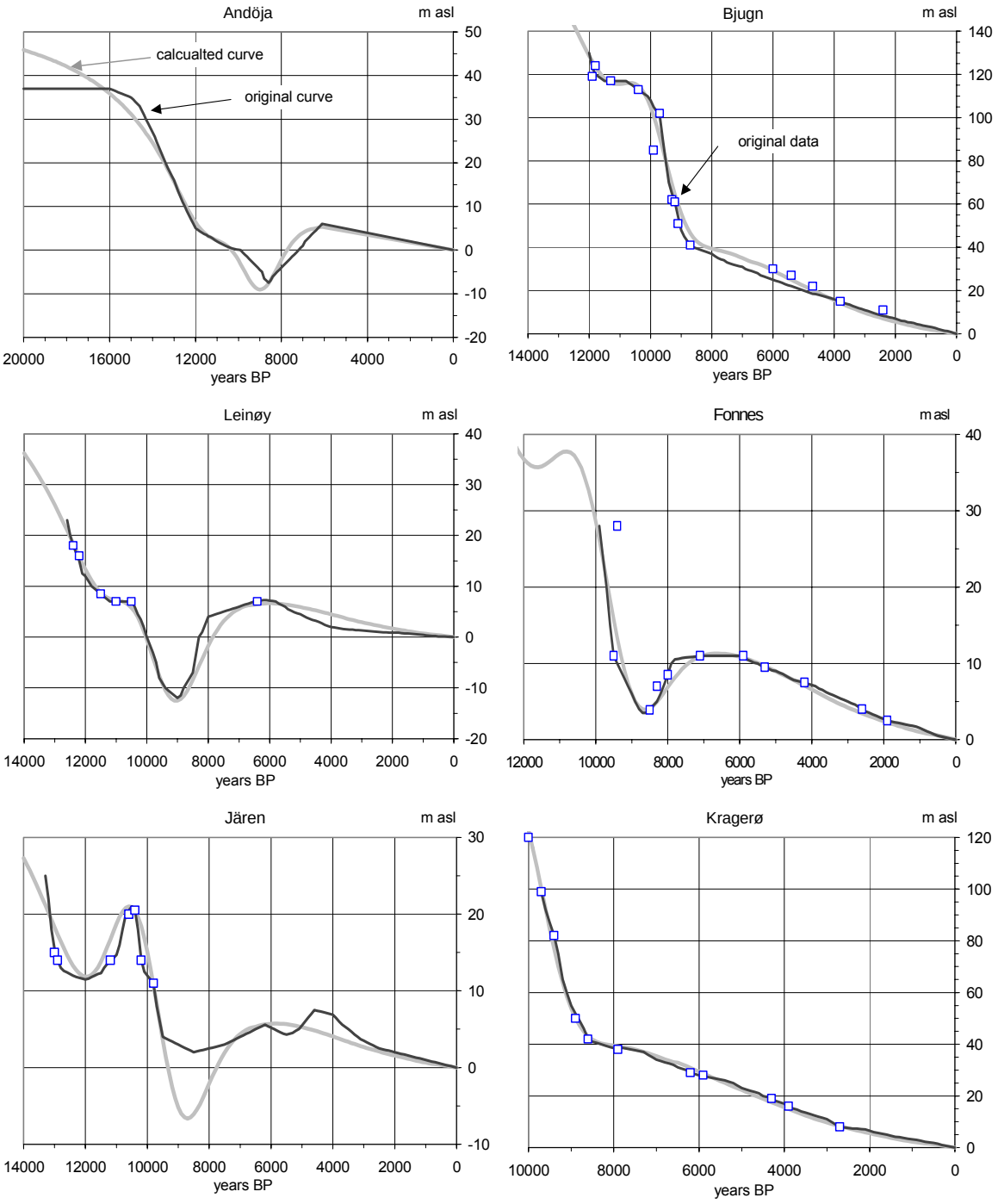

Figure 3-2. *Comparisons of original and calculated shore-level curves from Norway. For references see Table 3-1.*

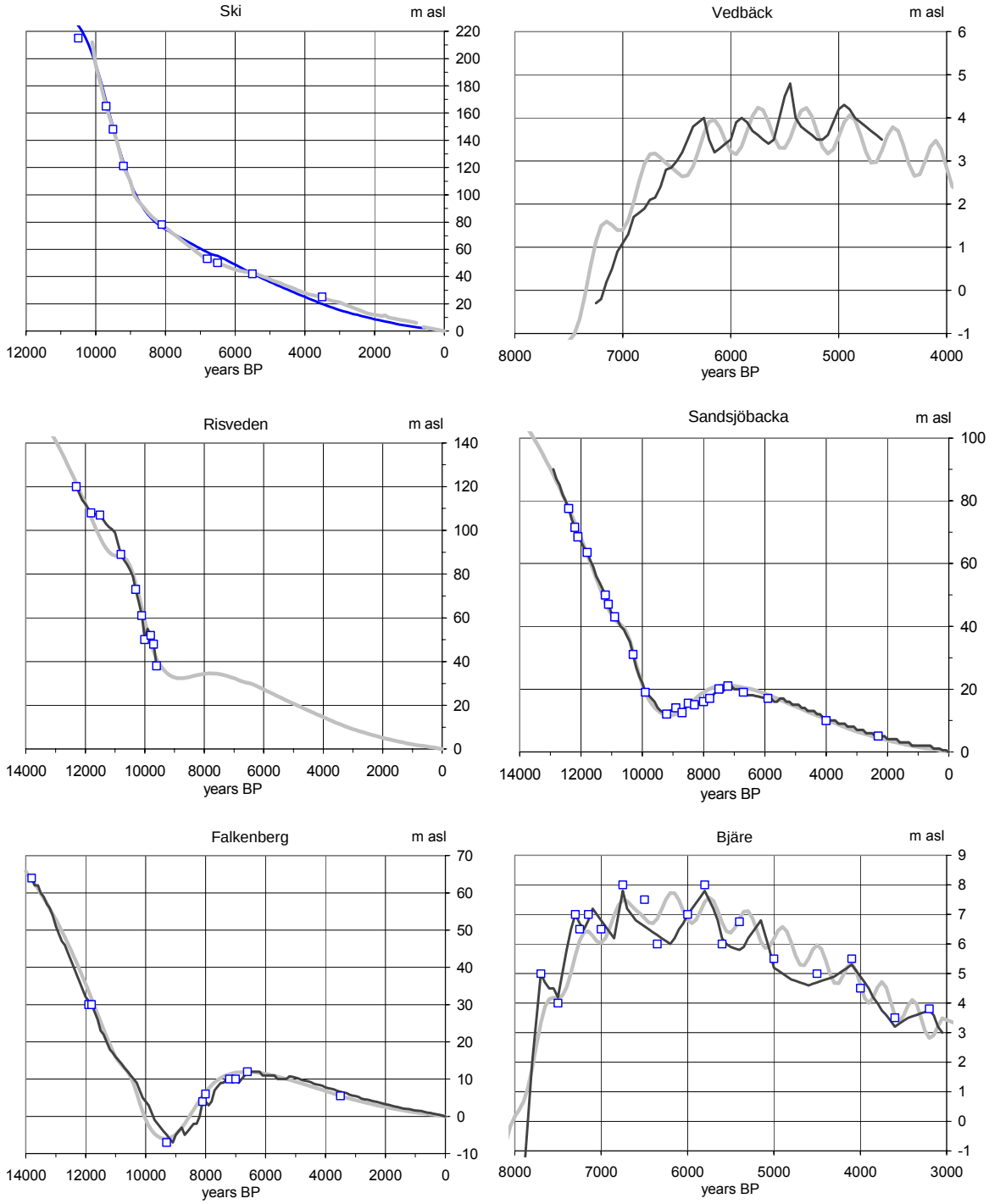

Figure 3-3. *Comparisons of original and calculated shore-level curves. For references see Table 3-1. The shore-level displacement at Vedbäck and at Bjäre is calculated with the oscillation formula included.*

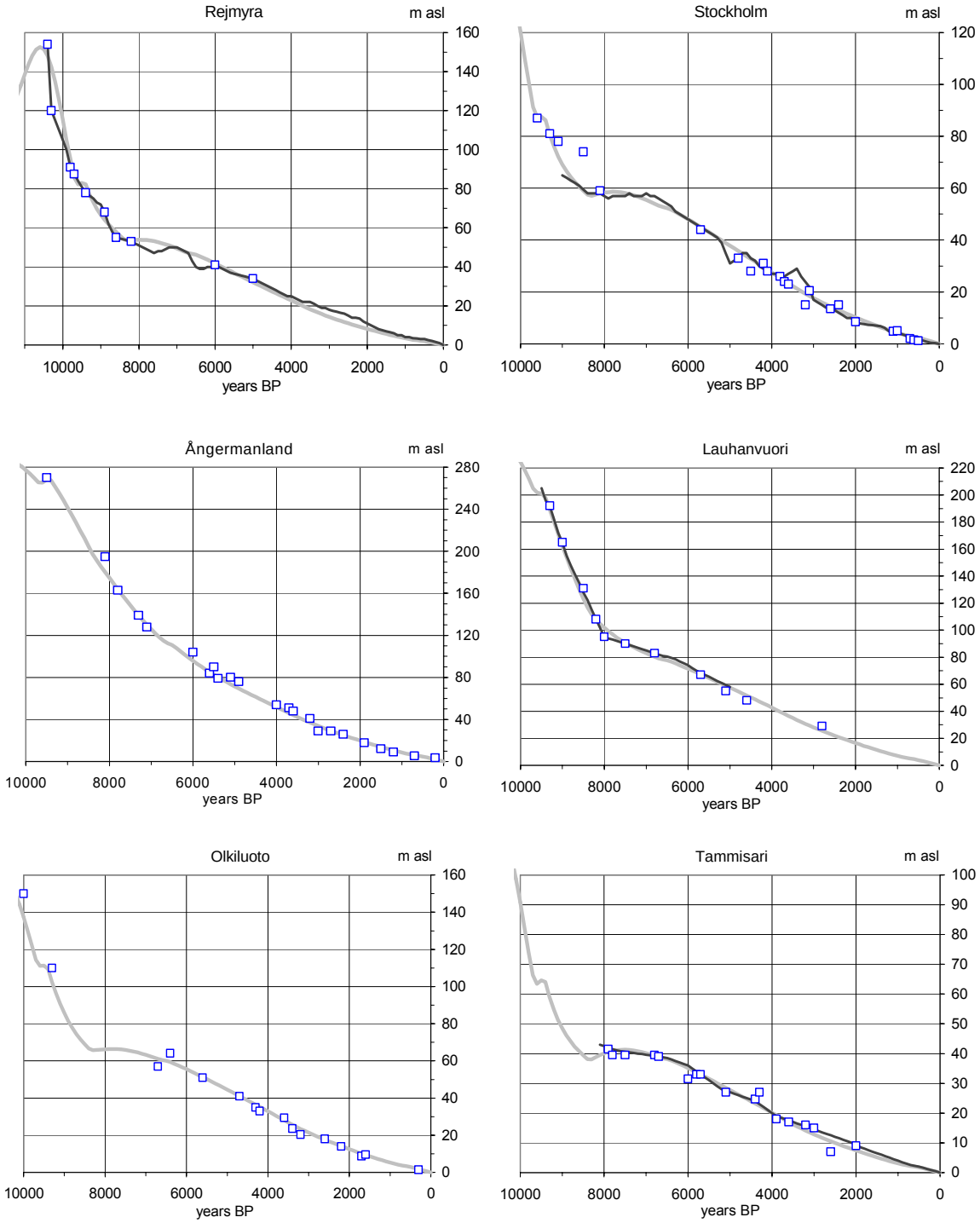

Figure 3-4. *Comparisons of original and calculated shore-level curves. For references see Table 3-1.*

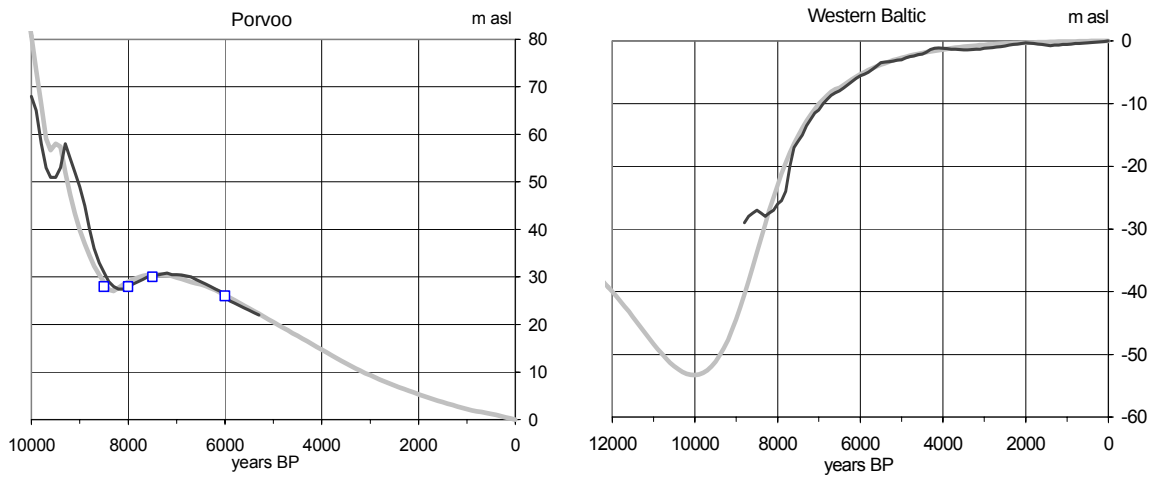

Figure 3-5. *Comparisons of original and calculated shore-level curves. For references see Table 3-1.*

3.2 Regional result

The estimated values of the A and B factors from the shore-level curves form the basis of the isoline maps, which are constructed in order to create an expression for the regional shore-level displacement. The configuration of the isolines, in all but one of the maps, is produced statistically by kriging. The maps constructed in this way, for the factors A_f, B_f and for B_s, are presented in Figure 3-6 to Figure 3-8. Initially kriging was used for constructing the map of A_s, Figure 3-9. Parts of this map indicates that the isolines are linear distributed. For that reason the A_s values were treated by linear triangulation in order to construct the isoline map, Figure 3-10.

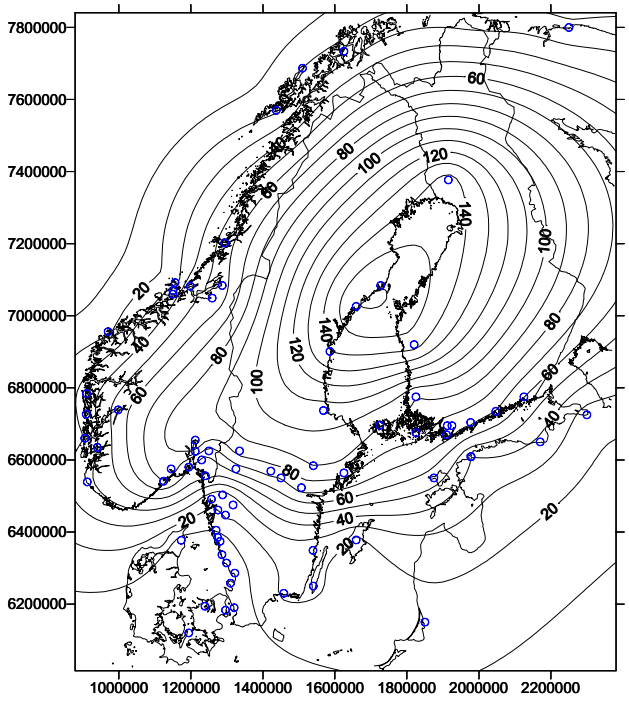

Figure 3-6. *Isoline map of A_f, i.e. total uplift/subsidence (m) for the fast component. The national Swedish grid system (in meter) is used as co-ordinates in the map.*

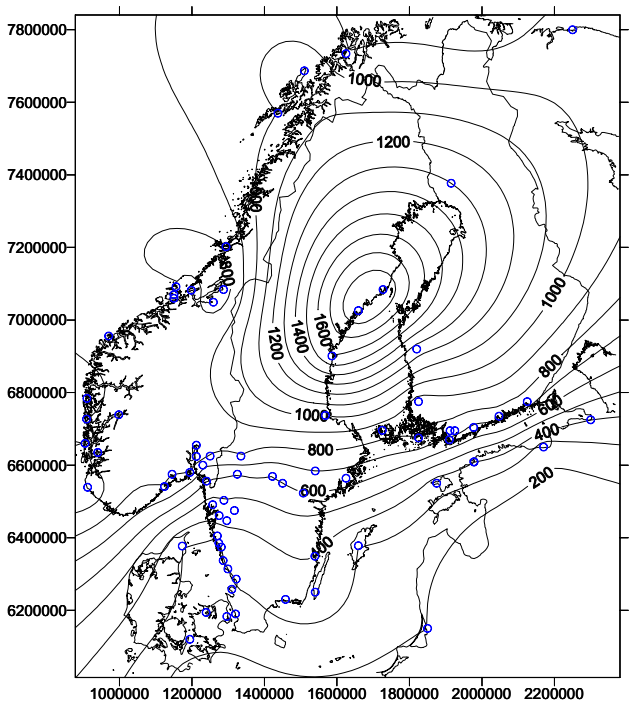

Figure 3-7. *Isoline map of B_f, i.e. the inertia factor (y^{-1}) for the fast component.*

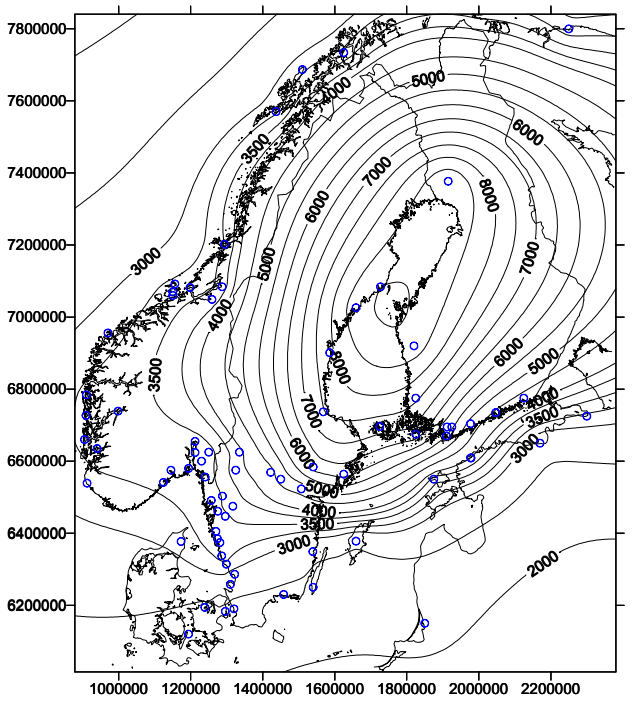

Figure 3-8. *Isoline map of B_s, i.e. the inertia factor (y^{-1}) for the slow component based on data from shore-level curves. Compare this map with Figure 3-12.*

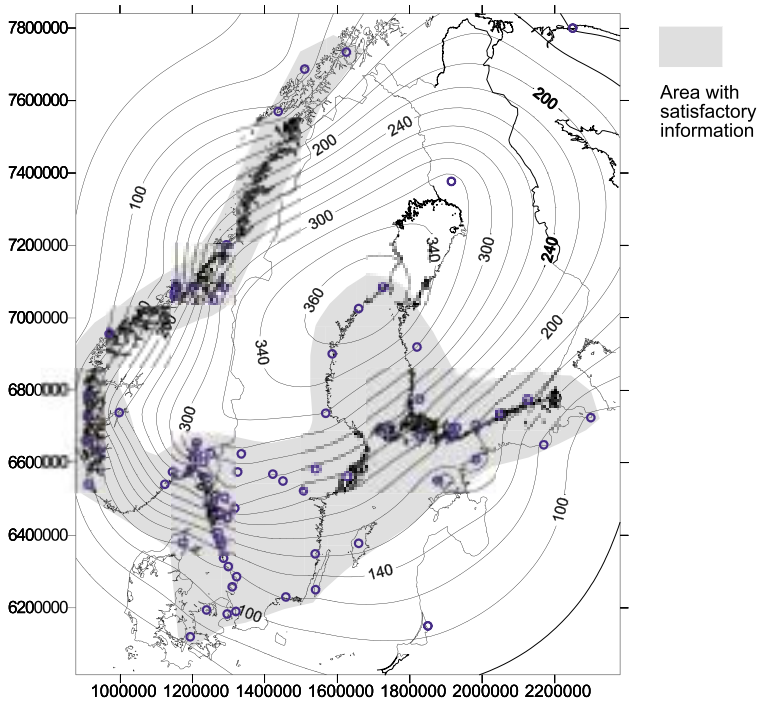

Figure 3-9. *Isoline map of A_s, i.e. the down load factor (m) for the slow component constructed by kriging and based solely on data from shore-level curves. The data used for constructing the isolines is unevenly distributed and there are vast areas where there is limited support for constructing isolines. Areas, where the isolines statistically are assumed to have been accurately constructed, are coloured. The configuration of the isolines in the coloured area indicates that the isolines are distributed in a linear pattern. Compare this map with Figure 3-10 and Figure 3-11.*

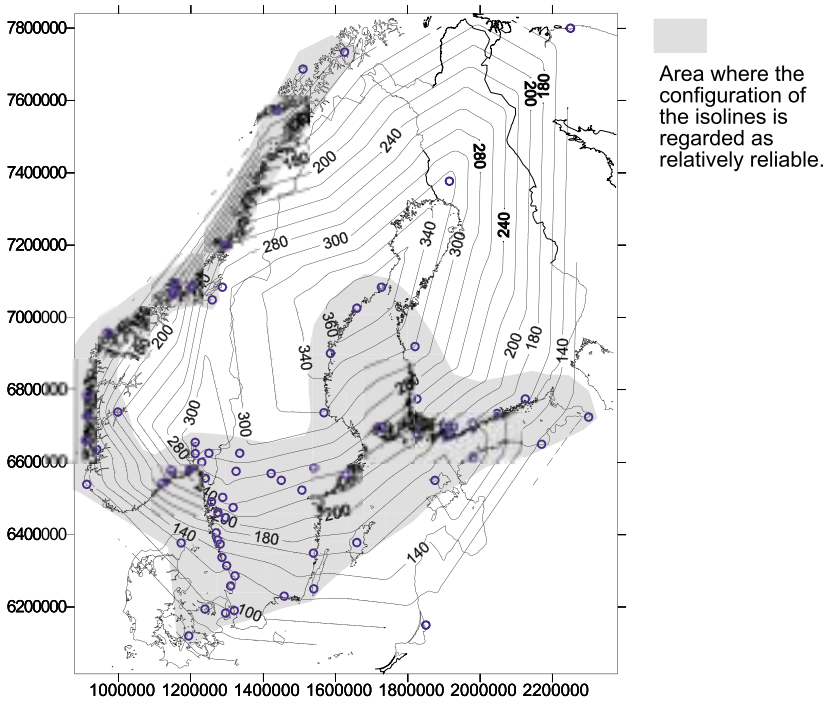

Figure 3-10. *Isoline map of A_s, the down load factor (m) for the slow component constructed by linear triangulation and based solely on data from shore-level curves. Compare this map with Figure 3-9 and Figure 3-11.*

The present uplift is only due to the slow component. That means that recent relative uplift can be calculated just from A_s and B_s. This is utilised for improving the maps of A_s and B_s. As these two factors are known at sites examined by the shore-level curves it is possible to interpolate the isoline configuration between these sites with great accuracy, by using the information of the recent uplift. The present eustatic rise is estimated at 1.1 mm/year in these calculations. Isoline maps of A_s and B_s constructed by shore-level information and the recent relative uplift are presented in Figure 3-11 and Figure 3-12.

There is considerable data on the relative recent uplift in Sweden and Finland. The accuracy of the isolines is therefore good over these two countries even for the inland parts. Recent relative uplift as a result of the modelling is presented in Figure 3-13. A special map of the relative recent uplift in Sweden, from RAK (1971) is shown in Figure 3-14. Comparisons to Figure 1-3, Figure 1-4 and Figure 3-14, which are maps of the empirical data of recent relative uplift, show great resemblance. However, notice that this is a circular argument as the maps of A_s and B_s are calculated from the data from the above mentioned maps.

There are small regional differences for T_f. These differences are summarised in Figure 3-15.

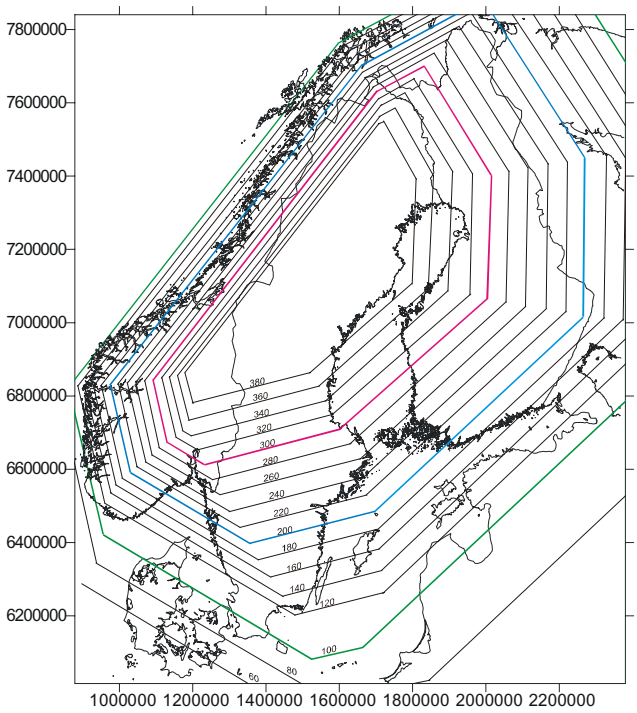

Figure 3-11. *Isoline map of A_s, i.e. the down load factor (m) for the slow component. This map is based on data from both shore-level curves and recent relative uplift and is regarded as the main result of the modelling. Compare this map with Figure 3-9 and Figure 3-11.*

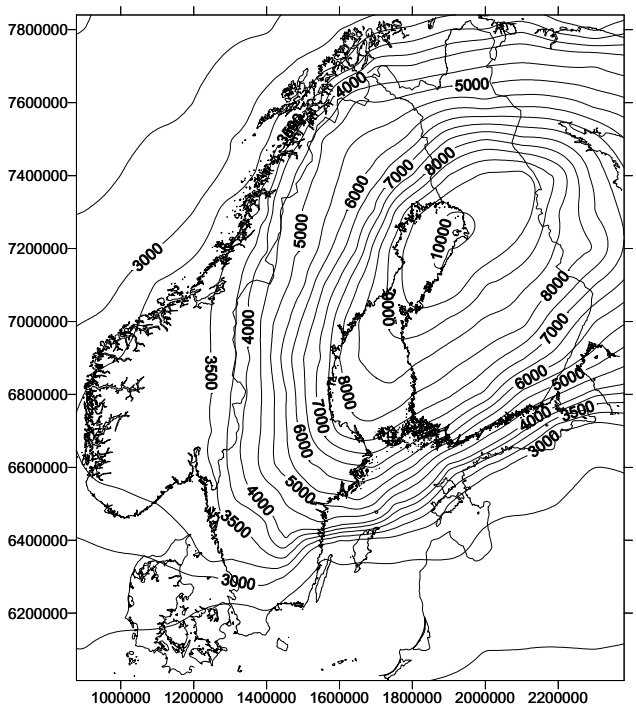

Figure 3-12. *Isoline map of B_s, i.e. the inertia factor (y^{-1}) for the slow component based on data from both shore-level curves and recent relative uplift. Compare this map with Figure 3-8.*

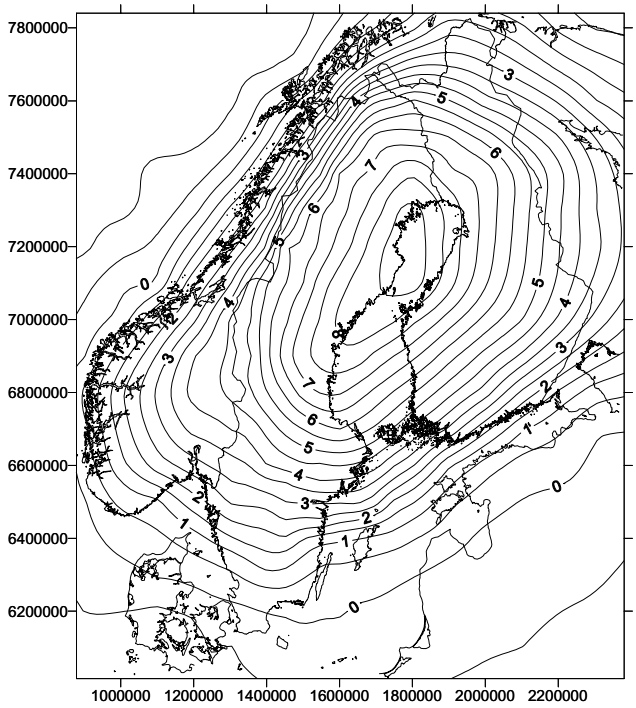

Figure 3-13. *Recent relative uplift as a result of the modelling. Comparisons to Figure 1-3, Figure 1-4 and Figure 3-14, which are maps of the empirical data of recent relative uplift, show great resemblance. However, notice that this is partly a circular argument as the maps of A_s and B_s are calculated from recent relative uplift.*

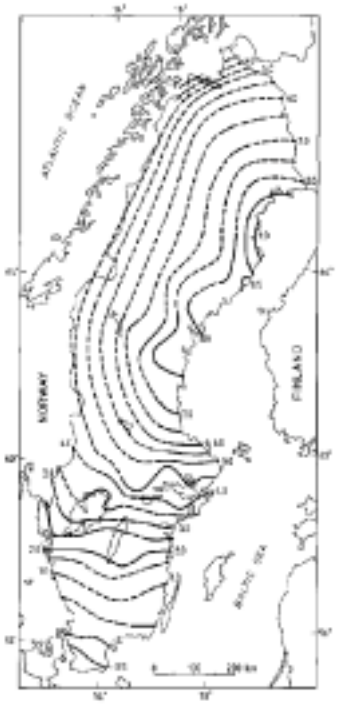

Figure 3-14. *Recent relative uplift in Sweden from RAK (1971).*

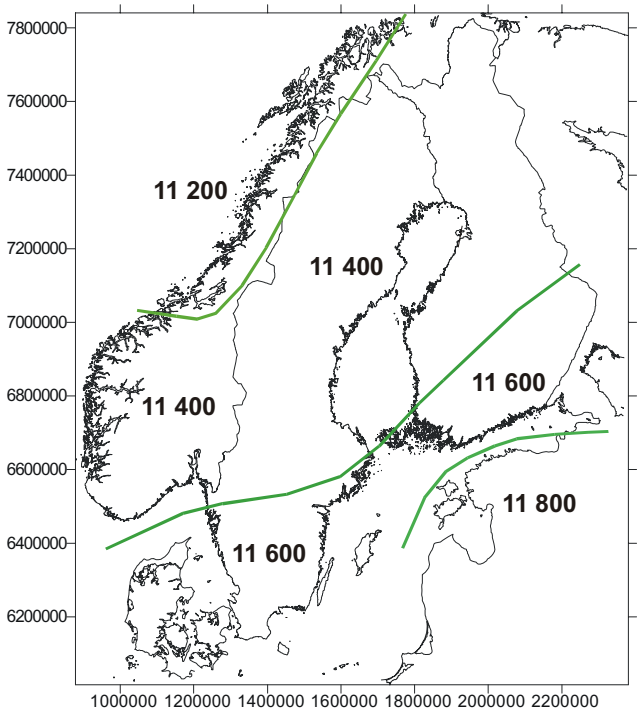

Figure 3-15. *Regional differences for T_f in cal years BP.*

4 Interpretation of the isoline maps

4.1 The inertia factor B_s

The present model shows a significant resemblance to the two earlier presented models (Påsse 1996b, 1997), but there are also notable differences. The understanding of the factor B_s, the inertia factor of the slow component, has increased during each new modelling. In the first modelling (Påsse 1996b) the existence of different inertia factors was established. In the second modelling (Påsse 1997) these differences were correlated to crustal thickness. In the present modelling the differences in the inertia factor are correlated to thickness of the lithosphere. This correlation gives plausible results as well as a more plausible explanation of the process. An interpretation of thickness of the lithosphere, according to analysis of wave data, has been presented by Ansorge et al. (1992), Figure 4-1. A comparison of the isolines of B_s to this map shows great resemblance. A correlation diagram, Figure 4-2, shows that there is a strong linear correlation between B_s and lithosphere thickness. The linear correlation between B_s and lithosphere thickness (L) can be expressed as:

$$L = 0.0014 \cdot B_s + 73 \qquad \text{Equation 4-1}$$

The values of B_s differ slightly from this trend in two areas. The southeastern part of Sweden shows somewhat lower values of the inertia factor. That means that thickness of the lithosphere probably is somewhat lower in this area, than was suggested by Ansorge et al. (1992). The opposite condition is valid for the southwestern part of Norway.

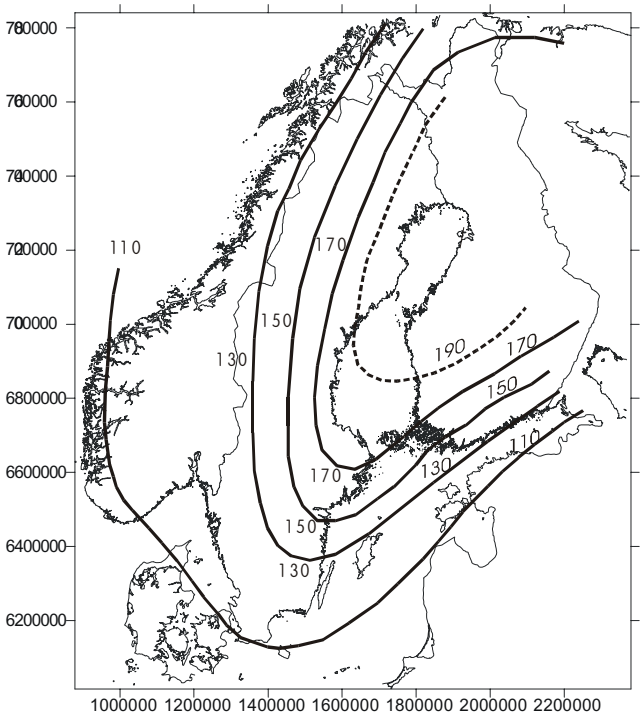

Figure 4-1. *Thickness of the lithosphere (km). Redrawn from Ansorge et al. (1992).*

Equation 4-1 is utilised for constructing Figure 4-3, where the B_s values from Figure 3-12 are transformed to lithosphere thickness. The two maps of lithosphere thickness (Figure 4-1 and Figure 4-3), constructed by different methods show great similarity.

Ekman & Mäkinen (1996) have proved, by repeated high-precision relative gravity measurements, that a viscous inflow of mantle material is a necessary part of the ongoing uplift process. Present uplift due to the slow component can thus be linked to viscous flow and a response to long-term stresses. There are several explanations of why areas with thick lithosphere are recovering more slowly than areas with thin lithosphere. One explanation may be that there is larger weight to elevate in areas with great lithosphere thickness. Another explanation may be that different thickness of the lithosphere implies differences in the thickness of the underlain viscous layer and that these differences affect the velocity of the viscous flow.

The glacio-isostatic uplift started at the same time as the ice started to be thinner. That means that a great part of the uplift occurred before the moment of the final local deglaciation, especially in central Fennoscandia. Due to the differences in the inertia factor the land below the ice sheet was uplifted non-uniformly. In the area around the Gulf of Bothnia the inertia factor, B_s, is relatively much higher than in other areas, and recovery in this area was thus delayed in comparison to other areas, for example central Norway. The non-uniformly uplift thus gradually changed the ice surface. Ice is assumed to have flown from areas with high uplift rate to areas with lower uplift in order to maintain the glacial balance. This mechanism may have produced a "glacial-tilting" analogous to the lake-tilting phenomenon. This hypothesis implies a self-triggered redistribution of the ice load during deglaciation. Glacial transgression may have caused local thickening of the ice sheet, which was compensated by isostatic subsidence or retardation, which in turn amplified the process. Climatic deterioration at about 11 000 years BP with a low deglaciation rate may have further amplified the process, by prolonging the period for glacial tilting.

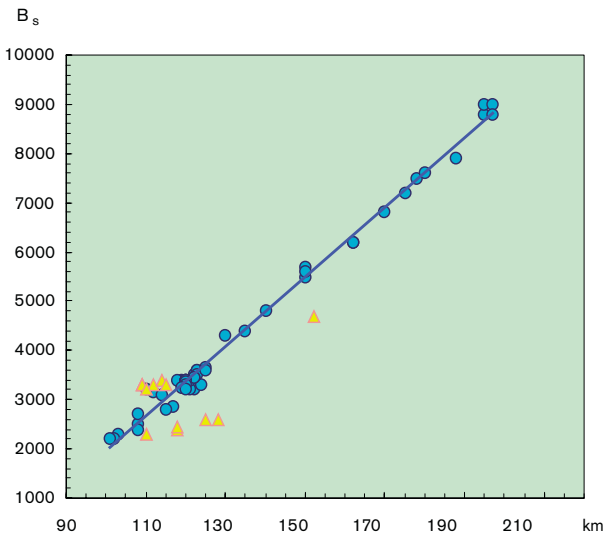

Figure 4-2. *There is a linear correlation between B_s and lithosphere thickness (L), which can be expressed as $L = 0.014\ B_s + 73$. The values from the southeastern part of Sweden and the south-western part of Norway, designated by triangles, are excluded in the calculation of the correlation.*

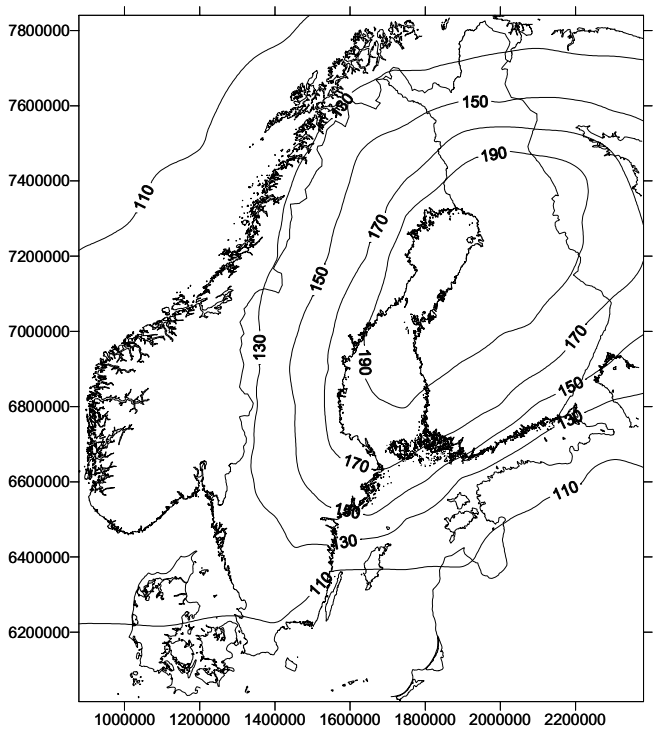

Figure 4-3. *Thickness of the lithosphere (km) as a result of the modelling. Compare this map with Figure 4-1.*

4.2 The pattern of crustal changes

The pattern of glacio isostatic recovery is visualised in a series of maps showing calculated levels of uplift at different times, Figures 4-4 to 4-6. A star in each map designates the most depressed area, which moves through time. At 16 000 years BP, when the recovery is assumed to have started, the crustal pattern is mainly affected by the ice-loading, i.e. the A_s factor. The most depressed area during this time is situated on the Scandinavian Highlands or more correctly at the eastern slope of the Highlands. From about 12 000 years BP a fast successive change of the position of the most depressed area from the Southwest towards the Northeast begins. Initially this change is mainly due to the fast component but since c. 9 000 years BP displacement of the most depressed area is due to the regional differences in the inertia effect. The recorded uplift in Figures 4-4 to 4-6 refers to the present sea level. However, the last map in Figure 4-6 is constructed in a different manner as uplift is related to a calculated future zero-level, which is reached when all isostatic movements are assumed to have ceased at 100 000 years AP. This map thus shows the total crustal recovery as a response to the latest glaciation. The maximal total uplift amounts to 600 m according to these calculations.

To sum up, the course of uplift could initially be described as mainly dependent of the A_s factor, later jointly dependent on the A_f and the B_f factors and finally dependent mainly on the B_s factor.

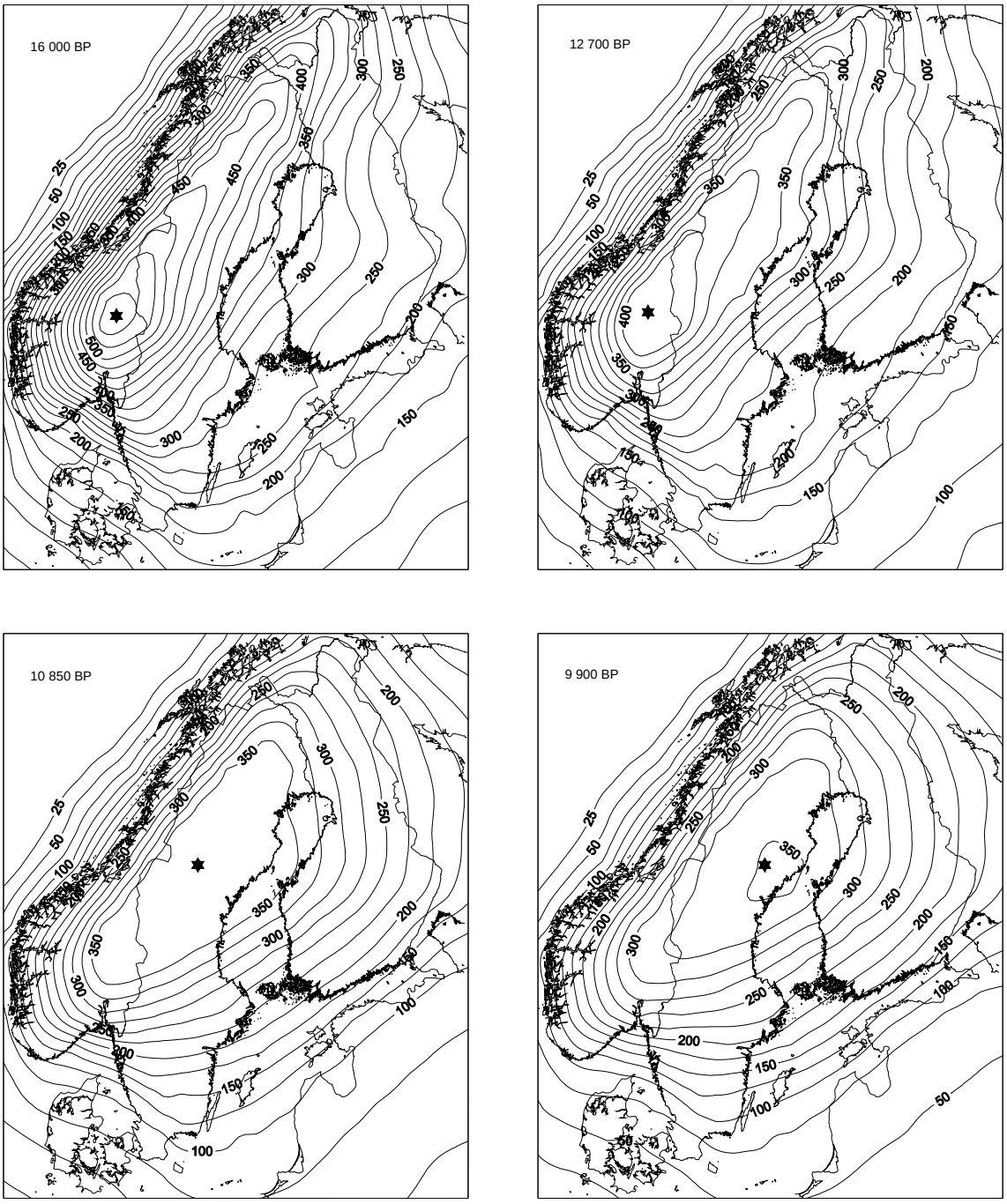

Figure 4-4. *Isolines of the calculated uplift (in m) at different times. The star designates the most depressed area, which changes successively toward the Northeast. Notice the large changes of the tilting direction for example in south central Sweden.*

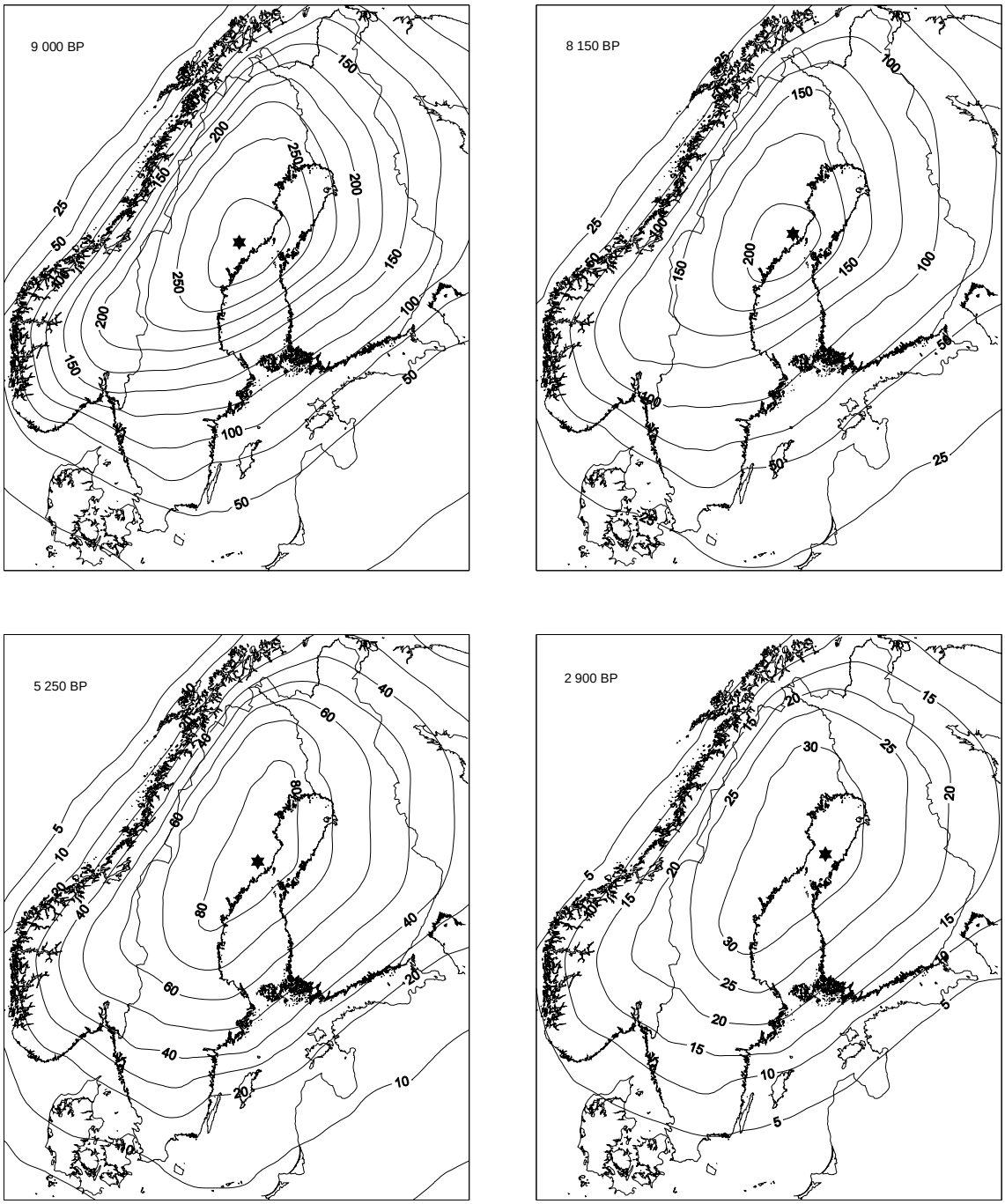

Figure 4-5. *Isolines of the calculated uplift (in m) at different times. The star designates the most depressed area at specific times.*

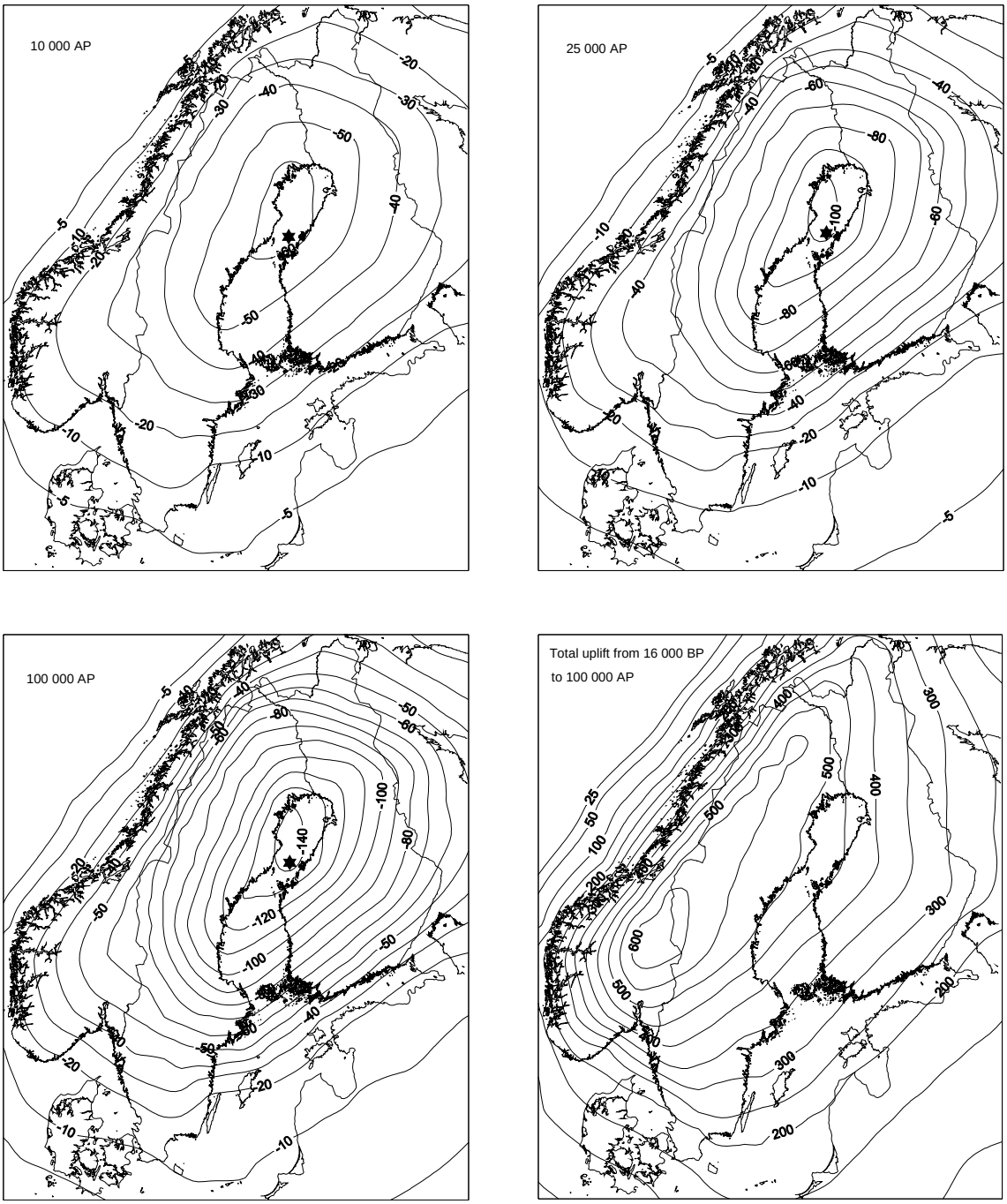

Figure 4-6. *Isolines of future remaining uplift (in m). AP designates years after present. The last map in this figure shows the total uplift from 16 000 years BP, when the glacio-isostatic recovery is assumed to have started, until 100 000 years AP, when recovery theoretically ceased.*

A discussion of the thickness of the Scandinavian ice sheet is consciously avoided in this report. One of the reasons for this is that the duration of the glacial load is very decisive for the amount of depression. A thick ice, existing only during a short period, may produce a small depression while thin ice, existing during a long period, may produce a similar or even bigger depression (Morén & Påsse 2001). Taken this into account it does not necessary mean that the ice had the greatest thickness in the Scandinavian Highlands even if this area was most depressed according to Figure 4-6. A just as good explanation is that this area has been covered by ice during a much longer period.

Figures 4-4 to 4-6 also show that there are extensive areas where the isolines are more or less parallel and evenly distributed. Between these areas there are narrow zones where the direction of the isolines or the gradient changes distinctly. The narrow zones extend both in radial and transverse directions from the uplift centre. This configuration of the isolines indicates a strong rigidity of the crust, which highly influences the uplift pattern by counteracting flexion of the crust. That means that glacio-isostatic movements occur in a linear manner by subsidence and upheaval of rigid plates and that the necessary crustal flexures involved in the glacio-isostatic movement occur in hinges. The hinges are most probably situated in pre-existing fault zones. Sauramo (1944) has earlier used the term hinge-line in a similar context.

The uplift pattern derived in the model indicates that the plates, where the isolines are more or less parallel and evenly distributed, are very extensive. However, such large extension of homogenous rigid plates is unlikely. Most probably the plates are divided into several small rock blocks, which more or less move in a similar manner within a specific plate (cf. Tirén et al. 1987, Tirén & Beckholmen 1988). The extension of the hinges cannot yet be accurately predicted by the results of the model.

Some of the rock blocks have had a more or less constant tilting direction while the direction of other rock blocks has changed considerably during the recovery. Rock blocks, where the tilting direction has changed considerably, are situated in areas where the isoline directions of A_s and B_s are in contrast (cf. Figures 3-8 and 3-11). The most prominent areas where A_s and B_s are in contrast are the southwestern half of southern Sweden (including the Oslo region), along the Swedish East Coast (north of the county of Uppland) and around the border between Sweden and Finland. The isolines of A_s and B_s are more-or-less perpendicularly distributed in these regions.

A connection may exist between the distribution of recent seismic events in Fennoscandia (e.g. Ahjos & Uski, 1992) and contrasting A_s and B_s isolines. This hypothesis implies that it is not necessarily the amount of crustal uplift or subsidence that is the main driving force for seismic activity. Instead changes of the tilting directions in and between the rock blocks are assumed to be the most important factor for creating glacio-isostatic induced seismic activity. The largest changes of the tilting directions occurred between 11 000 to 9 000 BP, which may well be the period when most large earthquakes occurred. The large postglacial neotectonic faults in the county of Norrbotten (Lagerbäck 1988, 1990), which are investigated in detail in several SKB projects, show activity within this time span.

The accepted view of the glacio-isostatic process is that the loading of ice produced a bowl-like depression in the crust. The conclusions from the present modelling may thus be regarded as controversial and thus need a thorough analysis. The first question to bring up for discussion is why the bowl-like depression is the accepted opinion? The consequent question is what information supports this opinion? The answer is that most isoline maps of ancient shorelines are generally drawn in a way that supports a bowl-like depression. This style of drawing the isolines started already in the late 19 century when the first shore-level observations were published (e.g. DeGeer 1888) and has since been

the common opinion. Smoothed curves were also used in the presentations of the recent relative uplift (Kääriäinen 1963, 1966, RAK 1971, 1974), which further "confirmed" the opinion of a bowl-like depression, Figure 1-3 and 1-4.

The smoothed curves in maps, showing ancient shore-levels and recent uplift velocities are commonly placed on an equal footing with the crustal subsidence/uplift. This association of ideas has been repeated so many times that most scientists regard it as a truth. What is forgotten, or not known, is that the levels of ancient shorelines or the velocities of the recent uplift are functions of the down load factor (*A*) **and** the regionally different inertia factor (*B*), besides the eustasy. That means that the inertia factor and the size of subsidence/uplift equally affect the configuration of shore level isolines. If this had not been the case, shore-level modelling would have been a simple task, as all sites with equal value of the recent relative uplift would have had an equal shore-level development. This is explicitly not the case.

Presentations of shore-level data in maps differ remarkably from presentations of shore-level data in diagrams. In so-called distance diagrams, shore levels from rather extended areas are plotted in the local tilting direction. These plot results are more or less exclusively in linear correlation to the shore-level observations (e.g. Mörner 1969, Anundsen 1985, Eronen et al. 1995). Påsse (1983) statistically investigated the linearity of isochronous shore-levels. Of importance in this context is that Mörner (1969), by plotting dated shore-levels from a vast area, found a bend (a hinge) in the linear distribution.

Why are shore-level observations, which are obviously linear in radial extension, presented by smoothed curves in transversal extension (in maps)? This inconsistency comes up when shore-level data from differently tilted rock blocks are combined and is most probably just a precaution. These comments are no scientific proof of transversal linearity but hopefully food for thought.

4.3 Time dependence of crustal changes

Morén & Påsse (2001) have extended the mathematical model presented by Påsse (1997) to be valid for the whole Weichselian glaciation, the Holocene and an assumed future glaciation. The extended model points out a causal connection within the glacio-isostatic development, which seems to have been neglected in most previous models. This causal connection is the strong time-dependence in the glacio-isostatic mechanism. Crustal uplift does not appear "momentary" but is markedly delayed due to the viscous flow mechanism and the flow velocity is concluded to be the main decisive factor for crustal changes. Movements, as a response to glacial loading, will thus most probably follow a similar movement such as unloading.

The thickness of the ice is important for creating the download. However, the viscous flow mechanism also implies that the **duration** of the glacial load is very decisive for the amount of depression. Thick ice, existing only for a short period, may produce a small depression while thin ice, existing for a long period, may produce a similar or even bigger depression. When the ice melts the uplift starts at the level of the depression. A "short-lived" glacial advance does not reach maximal isostatic balance during the download process as the depression is interrupted. This also implies that during the reverse movement, uplift usually ends at a level "far" from isostatic equilibrium. A conclusion from the extended modelling (Morén & Påsse 2001) is that there was most probably a relatively big "remaining" glacio-isostatic depression before the Late Weichselian maximum at c. 20 000 years BP.

In Equation 2-4 A_s is equal to the download at the time T_s. A_s determines the size of the depression and B_s determines the velocity. When considering the time dependence of the process of crustal changes, the values of A_s should not be interpreted to represent thickness of glacial ice. The A_s factor is perhaps better explained as the state of isostatic imbalance.

According to Figure 4-6 the Scandinavian Highlands was the most depressed area during the latest glacial maximum. Taken the time dependence of glacio-isostatic loading into account it does not necessary mean that the ice had the greatest thickness in the Scandinavian Highlands during this time. A just as good explanation is that this area was covered by ice during a much longer period than the remaining Fennoscandia.

4.4 A_f and B_f

The configuration of the A_f isolines shows a pattern quite similar to the ice recession, Figure 4-7. The fast component is restricted in time to the two latest phases in the deglaciation pattern, i.e. to the regeneration of the inland ice during the Younger Dryas time (and partly Alleröd time) and to the final disappearance of the ice during the early Holocene period. It can thus be concluded that the fast component is connected to the latest part of the deglaciation. According to the shore-level development the glacial regeneration lasted about 2 000 years. This is a deviation from the accepted opinion, that retardation in the deglaciation or a re-advance is said to have occurred only during the last 700 years of the Late Weichselian.

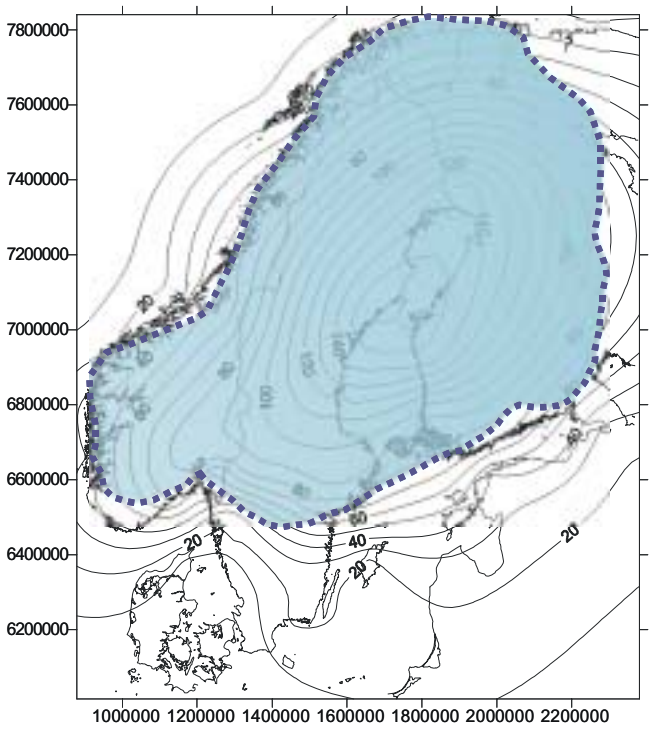

Figure 4-7. *The extension of the Scandinavian ice about 10 300 years BP in comparison to the A_f isolines.*

The asthenosphere is assumed to exhibit plastic behaviour. This means that when the asthenosphere encounters long-term stresses, the material within it will flow. However, in response to short-lived stresses it behaves like elastic solid. The slow component is most probably due to viscous flow in the asthenosphere and the fast component is assumed to be due its elasticity. Fjeldskaar (2000) recently discussed the elastic component in the glacio-isostatic process and concluded that the elastic deflection would be insignificant to simulate postglacial uplift in models. However, this conclusion seems to be deduced only from elasticity of the lithosphere.

Crustal subsidence, which reached its maximum around 10 300 years BP (11 400 cal years BP), is hardly possible to explain in another way than reloading of the crust in the central parts of Fennoscandia. Of importance for the interpretation is that areas situated far away from the ice margin were subsided. This subsidence can be explained by the rock block hypothesis, which implies that changes of the total load upon a rock block determine the crustal changes and as the block is rigid the whole block is affected by the load. When the load is unevenly distributed it will produce a tilt of the block. This mechanism can be seen as a form of buoyancy, where proximal reloading of a separate block produced subsidence and tilting of the whole block in sympathetic motions. When the proximal part of the block was later unloaded this gave rise to sympathetic uplift in the distal part. The velocity of uplift in the distal part is then determined by the total motion of the block and could, for that reason, be very fast. The rate of uplift in areas situated more closely to the ice margin was accordingly slower. This is also confirmed in the results of the modelling, where the values of B_f are much lower in distal parts then in proximal parts, Figure 3-7. The velocity of the ice recession during the uplift phase of this event is also mirrored in the values of B_f. Areas with low ice recession velocity, e.g. along the West Coast of Norway, have thus high values of B_f. The small differences in the values of T_f are explained in a similar way due to the recession velocity following the deglaciation during the early Holocene, Figure 3-15.

So far, only the development outside the Younger Dryas ice border has been discussed. However, the fast component is even greater in the area inside the Younger Dryas ice border. The explanation for the fast component given above is based on a buoyancy mechanism involved in glacio-isostatic movements. This is most probably the explanation of the fast component even inside the Younger Dryas ice border. As shore-level curves do not give any information of crustal changes before 10 300 years BP in this area it is impossible to make univocal conclusions regarding the subsidence phase. However, pronounced subsidence (or more correctly retardation) is observed close to the ice margin. For that reason it is most likely (and is also predicted by the rock block hypothesis) that similar crustal movements occurred in ice covered areas. However, there is a noteworthy difference as there are differences in the deglaciation development between the areas inside and outside the Younger Dryas border. The area situated inside the border was most likely covered by relatively thick ice during Younger Dryas time and partly during the early Holocene period. The “buoyancy effect” was thus much greater within this area.

The isoline map of A_f is derived solely from the factors received as a result of the shore-level curve calculations. The configuration of the curve is estimated by kriging. According to the rock block hypothesis the map of A_f ought to have been constructed by a linear treatment. However, available data are not sufficient to produce a reliable map by this treatment. For that reason A_f is reported here by smoothed curves, Figure 3-6. However, there are configurations in the A_f map, which suggest linearity. If the blocks from the A_s map were used as an answer it would be possible to construct a rough linear picture of the A_f isolines. However, the direction of the A_f isolines most probably differ from the direction of the A_s isolines.

5 The Baltic

The accepted model of shore-level development in the Baltic comprises two lake phases, the Baltic Ice Lake and the Ancylus Lake. These two lake phases were each followed by marine phases, the Yoldia Sea and the Littorina Sea. Research into the development of the Baltic Sea since the last deglaciation has resulted in an immense number of publications. A review of this topic is presented by Björck (1995), which contains most of the relevant references regarding the development of the Baltic Sea.

According to current opinion the Baltic Ice Lake was dammed by c. 25 meters and is assumed to have been drained during a catastrophic event, at Mt. Billingen at c. 10 300 years BP. Several drainage sites have been suggested, but also questioned, as the traces of this huge drainage do not show sufficient evidence. Lakes at different altitudes, which are assumed to have been isolated at approximately the same time, have been used to demonstrate the drainage of the Baltic Ice Lake (Berglund 1966, Björck 1979, Svensson 1989). The isolation of these lakes occurred around 10 300 years BP. However, a similar course of shore-level displacement also occurred at the Swedish West Coast. Svedhage (1985) has discussed this similarity in the shore-level development between the Swedish West Coast and southeastern Sweden. He concludes that the mechanism of the fast regression was due to crustal changes and thus not should be linked to drainage of the Baltic Ice Lake. This conclusion is confirmed by the results of this work.

According to the modelling, glacio-isostatic uplift and thus shore-level displacement was extremely rapid due to the fast component around 10 300 years BP. Before the fast uplift there was a period of fast subsidence related to the fast component. This crustal development is recorded in shore-level curves from the Norwegian West Coast and named the Younger Dryas transgression by Anundsen (1985). At the Swedish West Coast the fast crustal subsidence is not mirrored as a transgression but in a period of slow regression followed by a period of very fast regression. Similar crustal changes, which gave the Younger Dryas transgression, are demonstrated within the Baltic basin by the modelling.

It is always hard to present a new interpretation contradicting a common opinion. In this special case it is especially inconvenient as shore-level curves from the Baltic are constructed with the presumption of an existing drainage of the Baltic Ice Lake. However, there are three sources of errors involved in the determinations of the isolations of lakes contemporary with the drainage of the Baltic Ice Lake and thus in the construction of sea-level curves, which should not be neglected.

- The isolation of a lake from the Baltic Ice Lake means no change in salinity of the water.
- The isolation occurred during a very pronounced climatic and vegetational change.
- The isolations used in the shore-level curves are dated by pollen analysis. Pollen analytical dating can rarely be done more accurately then ± 100 years.

Six shore-level curves, which comprising the “drainage” event are shown in Figure 5-1. Björck (1979) empirically records a transgression before a fast regression in the shore-level curve from Blekinge. This transgression is confirmed in the model and also recorded at St Petersburg (Dolukhanov 1979), at Narva and at Tallinn (Kessel & Raukas 1979), Figure 5-1.

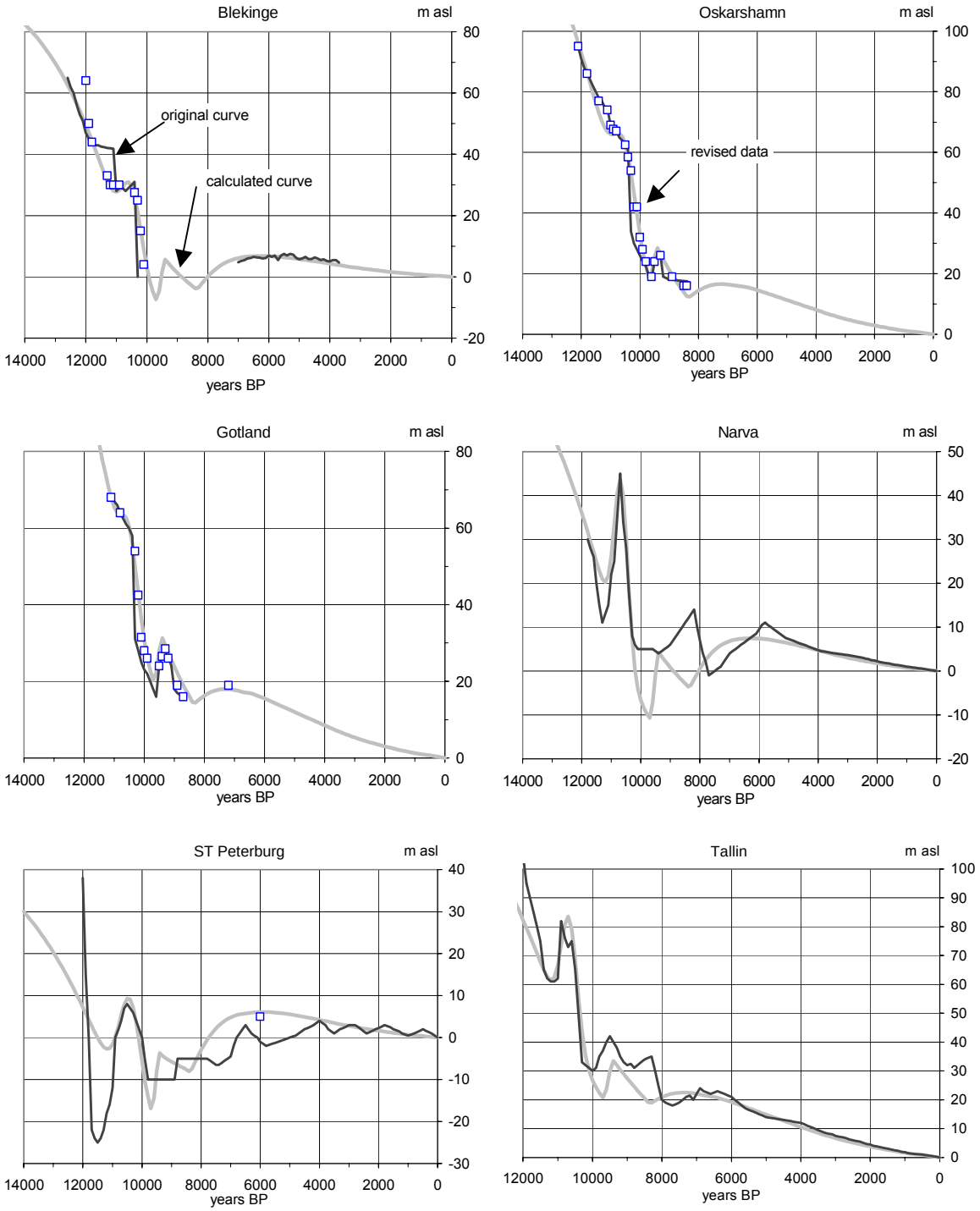

Figure 5-1. *Shore-level curves from the Baltic. In the original curves shore-level displacement is interpreted as a drainage around 10 300 years BP. In the calculated curves shore-level displacement during this period is interpreted as regression due to the fast component. In four of the curves this fast regression is preceded by a transgression. The original pollen analytical dates at Blekinge, Oskarshamn and Gotland are revised in this figure. This is done in order to show how small the revisions need to be to give another interpretation of the shore level displacement. The revisions never exceed ± 200 years and for most sites stay at ± 100 years.*

The source of errors indicates the difficulties involved in constructing shore-level curves for the actual period in the Baltic basin. The model predicts duration of the fast regression, "the drainage", to be about 400 years, while shore-level curves from the Baltic basin are drawn with the assumption of a momentary regression. Because of this the calculated shore-level curves do not exactly fit the existing shore-level curves in this area. If the original pollen analytical dates at Blekinge, Oskarshamn and Gotland are revised it is possible to get a good correlation of these dates to the calculated curves. The revisions, shown in Figure 5-1, never exceed ± 200 years and for most sites stay at ± 100 years. That means that the course of the "drainage" falls within the confidence interval for the pollen analytical dates. This revision indicates that the existing shore-level curves not by them self can be used as proof of the drainage.

Following the deglaciation there were initially two outlets from the Baltic as in present time, through the Great Belt and through the Öresund straits. The Great Belt emerged at roughly 12 000 years BP. During the later part of Late Weichselian the drainage of the Baltic was thus only through the Öresund strait. This outlet was narrow and at the end of Younger Dryas, very shallow. These conditions created an Inland Sea with fresh water. These conditions were also strengthened by the fact that the Baltic received a huge mass of melt water from the vanishing ice sheet during this period. However, as the Baltic was at the same level as the sea during this period, this phase should be regarded as a sea phase and not as an ice lake. Nilsson (1968) has earlier proposed a sea facies at the beginning of the development of the Baltic, which he names the **Baltic Ice Sea**. This name is here suggested to be extended and to be valid as a name for the initial phase of the Baltic.

After the Baltic Ice Sea followed a somewhat more marine phase where new connections from the Baltic to the ocean flow through the Vänern Basin. This phase is named the **Yoldia Sea** and lasted about 800–1 000 years. Due to the crustal uplift there was a fast gradual lowering of the connection between the Baltic and the sea. The Yoldia Sea thus became an Inland Sea during the latter part of this stage. This stage ended when the threshold at Degerfors emerged shortly before 9 600 years BP.

A very fast transgression, the Ancylus transgression, started in the Baltic when the threshold at Degerfors emerged and the Svea River drained the Baltic. The threshold at Degerfors is situated at approximately c. 105 m above sea level and the marine shore-level is calculated to have passed this level shortly before 9 600 years BP. In the model the rise of the threshold at Degerfors can be calculated with A_s = 260, B_s = 4300, A_f = 75, T_f = 11 500 and B_f = 600 and water level within the **Ancylus Lake** follows this rise, Figure 5-2.

When the water level, after a transgressive phase of about 200 years, reached a level of about 16 meters a new outlet, through the Great Belt, opened in the southern part of the Baltic. This alteration of the outlet occurred about 9 400 BP, a date which also represents the maximum of the Ancylus transgression. After this maximum the water level of the Baltic decreased in phase with the shore-level displacement at the Darss Sill. This stage of the development of the Baltic may be named the Ancylus regression. The threshold at Darss Sill was reached by the marine transgression at about 8 300 BP, Figure 5-2. This date defines the end of the Ancylus Lake.

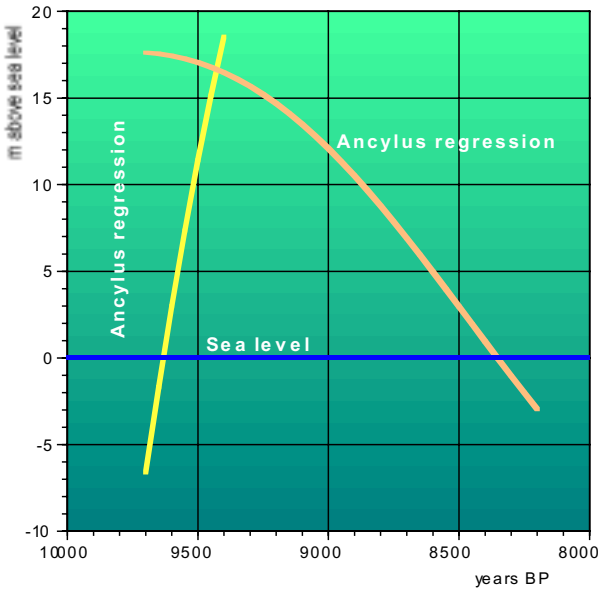

Figure 5-2. *The water level changes during the Ancylus Lake are estimated by combining the results of the calculated shore-level displacements at the outlets at Degerfors (Svea River) and at Darss Sill. The Ancylus transgression followed the emergence of the outlet at Degerfors (yellow). After that the outlet at Darss Sill was reached by the transgression the water level of the Baltic decreased in phase with the shore-level displacement at Darss Sill (orange). The calculated values of the water level in the Ancylus Lake are implemented in the model.*

When the sea intruded the Baltic through the Great Belt (Storebält) the Baltic was once again on the same level as the sea. This phase of the Baltic is named the **Littorina Sea**. The initial phase of the Littorina Sea is commonly considered to be a separate stage, the Mastogloia Sea. This sub-stage is defined by brackish conditions, caused by the shallow connections between the sea and the Baltic during this time. About 1 000 years later a connection to the sea also opened through the Öresund strait, giving more marine conditions within the Baltic.

6 Test and improvement of the model

One way of testing the model is to use the same method for another formerly glaciated area. By such an investigation it would be possible to confirm or reject the correlation between the inertia factor and thickness of the lithosphere.

One of the main results of the model is the rock block hypothesis. This hypothesis would be possible to test by a variety of investigations. One of these investigations could be a test of linearity of ancient shore-levels along the Swedish East Coast and along the coast of Finland. It would also be possible to get data for testing the linearity within inland areas by levelling shore marks above the present lake level in tilted lakes. However, the simplest method for testing linearity would be to closely analyse the accessible and comprehensive information of the present relative uplift. Presumably this analysis would give further evidence of the differentiation in rock blocks.

If the block hypothesis is accepted it would be possible to improve the model by introducing the spatial information of basement tectonics in the model.

7 Summary

The objective is to find mathematical expressions that describe shore-level displacement and glacio-isostatic uplift in the area covered by Scandinavian ice during the Weichselian glaciation. As the mathematical expressions are strictly empirical, they can be used for evaluations of both geological and geophysical parameters involved in the glacio-isostatic process. The model is purely empirical while most other models are based on more or less well-supported assumptions about ice thickness, deglaciation rates and geophysical parameters. The author, in SKB Technical Reports (1996b, 1997), presented two mathematical models of shore-level displacement in Fennoscandia. Utilising information about relative recent uplift from precision levelling extends this third modelling.

Shore-level displacement (S m) in Fennoscandia is mainly due to two interactive vertical movements, glacio-isostatic uplift (U m) and global eustatic sea level rise (E m), where $S = U - E$.

Påsse (1990a, 1996a, 1998) investigated glacio-isostatic uplift based on the lake-tilting method. By magnifying the function, which describes the lake-tilting, it has been possible to start an iteration process that has given mathematical expression for factors involved both within the isostatic movements and the eustatic rise.

The main input data, besides the lake-tilting information, are 72 shore-level curves from the area covered by Scandinavian ice during the Late Weichselian. Shore-level curves are compared to iterative calculated curves derived from the mathematical expressions. Information concerning present relative uplift (mm/y), recorded by precision levelling and tide gauge data, has also been used.

There are two components involved in glacio-isostatic uplift. The main uplift, still in progress, acts slowly. This component is called the slow component. During the end of the deglaciation there was another component involved in the crustal changes. This component gave rise to fast crustal changes of short duration and is called the fast component.

Land uplift following unloading of ice (U_s in m) can be described with the function:

$$U_s = \frac{2}{\pi} \cdot A_s \cdot \left[\arctan\left(\frac{T_s}{B_s} \right) - \arctan\left[\left(\frac{T_s - t}{B_s} \right) \right] \right]$$

where A_s is the download factor (m), which is the depression at the time T_s (years), which is the symmetry point of the function, t (year) is the variable time and B_s (y^{-1}) is an inertia factor. In the calculations T_s and t are counted in calendar years. The factors A_s and B_s differ regionally while T_s seems to be regionally constant and is estimated to 12 000 calendar years BP i.e. 10 850 years BP counted in the conventional radiocarbon chronology.

Shore-level curves from areas outside the Younger Dryas ice border show crustal subsidence or retardation during Alleröd and Younger Dryas time, followed by fast uplift during early Holocene. Fast uplift lasted at some sites about 1000–2000 years but was

usually of much shorter duration. Fast uplift during early Holocene is especially significant in central Fennoscandia and recorded in all shore-level curves from this area.

A general formula for the fast component is:

$$U_f = A_f \cdot e^{\left[-0.5\cdot\left(\frac{t-T_f}{B_f}\right)^2\right]}$$

where U_f is the crustal change (m), A_f is the total subsidence/uplift (m), B_f is the inertia factor (y^{-1}), t is the variable time (year) and T_f is the time for the maximal subsidence/uplift, i.e. the symmetry point of the function. T_f has small regional differences and varies between 11 800 to 11 200 cal years BP (10 700 to 10 100 years BP).

By calculating the difference between hypothetical uplift curves and empirical shore-level curves it has been possible to estimate a function for the eustasy:

$$E = \frac{2}{\pi}\cdot 56 \cdot \left[\arctan\left(\frac{9500}{1350}\right) - \arctan\left[\left(\frac{9500-t}{1350}\right)\right]\right]$$

The factors, estimated from the shore-level curves, form the basis of the isoline maps, which are the framework in the model. The configuration of the isolines, in all but one of the maps, is produced statistically by kriging. Initially kriging was used for constructing the map of A_s, but as this map indicates that the isolines are distributed in a linear pattern the A_s isolines were constructed by linear triangulation.

The present uplift is only due to the slow component. That means that recent relative uplift can be calculated just from A_s and B_s. This is utilised for improving the maps of A_s and B_s. As these factors are known at sites, examined by the shore-level curves, it is possible to interpolate the isoline configuration between these sites with great accuracy by using the information of the recent uplift, Figure 3-11 and Figure 3-12.

A strong linear correlation between the inertia factor B_s and lithosphere thickness has been found in the model. There are several plausible explanations of why areas with thick lithosphere are recovering more slowly than areas with thin lithosphere. One explanation may be that there is larger weight to elevate in areas with great lithosphere thickness. Another explanation may be that different thickness of the lithosphere implies differences in the thickness of the underlain viscous layer and that these differences affect the velocity of the viscous flow.

The pattern of glacio-isostatic recovery is visualised in a series of maps, Figure 4-4 to 4-6. These maps show that the most depressed area moves through time. At 16 000 years BP, when the recovery is assumed to have started, the crustal pattern is mainly affected by the ice-loading pattern, i.e. the A_s factor. The most depressed area during this time is situated on the Scandinavian Highlands. From about 12 000 years BP a fast successive change of the position of the most depressed area from the Southwest towards the Northeast begins. Initially this change is mainly due to the fast component but since c. 9 000 years BP displacement of the most depressed area is due to the regional differences in the inertia effect.

The pattern of glacio-isostatic recovery also shows that there are extensive areas where the isolines are more or less parallel and evenly distributed. Between these areas there are narrow zones where the direction of the isolines or the gradient changes distinctly. This configuration of the isolines indicates a strong rigidity of the crust, where glacio-isostatic movements occur in a linear manner by subsidence and upheaval of rigid plates and that the necessary crustal flexures involved in the glacio-isostatic movement occur in hinges. The hinges are most probably situated in pre-existence fault zones. Most probably the plates are divided into several small rock blocks, which more or less move in a similar manner within a specific plate. The extension of the hinges cannot yet be accurately predicted by the results of the model.

Some of the rock blocks have had a more or less constant tilting direction while the direction of other rock blocks has changed considerably during the recovery. Rock blocks, where the tilting direction has changed considerably, are situated in areas where the isoline directions of A_s and B_s are in contrast (cf. Figures 3-8 and 3-11). The most prominent areas where A_s and B_s are in contrast are the southwestern half of southern Sweden (including the Oslo region), along the Swedish East Coast (north of the county of Uppland) and around the border between Sweden and Finland. The isolines of A_s and B_s are more-or-less perpendicularly distributed in these regions.

A connection may exist between the distribution of recent seismic events in Fennoscandia (e.g. Ahjos & Uski 1992) and contrasting A_s and B_s isolines. This hypothesis implies that it is not necessarily the amount of crustal uplift or subsidence that is the main driving force for seismic activity. Instead changes of the tilting directions in and between the rock blocks are assumed to be the most important factor for creating glacio-isostatic induced seismic activity.

The configuration of the A_f isolines shows a pattern quite similar to the ice recession. The fast component is restricted in time to the two latest phases in the deglaciation pattern, i.e. to the regeneration of the inland ice during the Younger Dryas time (and partly Alleröd time) and to the final disappearance of the ice during the early Holocene period. Crustal subsidence, which reached its maximum around 10 300 years BP, is hardly possible to explain in another way than reloading of the crust in the central parts of Fennoscandia. Of importance for the interpretation is that areas situated far away from the ice margin were subsided. This subsidence can be explained by the block hypothesis, which implies that changes of the total load upon a block determine the crustal changes and as the block is rigid the whole block is affected by the load.

The slow component is most probably due to viscous flow in the asthenosphere and the fast component is assumed to be due to its elasticity.

The accepted model of shore-level development in the Baltic comprises two lake phases, the Baltic Ice Lake and the Ancylus Lake. The Baltic Ice Lake is assumed to have been dammed by c. 25 metres and drained during a catastrophic event, at Mt. Billingen at c. 10 300 years BP. According to the calculations, glacio-isostatic uplift and thus the regressive shore-level displacement was extremely rapid around 10 300 years BP. This fast regression was contemporaneous and occurred in a similar way at the West Coasts of Norway and Sweden as well as in the Baltic. The “drainage” of the Baltic Ice Lake has been reinterpreted in the model as due to crustal changes due to the fast component.

8 References

Ahjos T & Uski M 1992. Earthquake in northern Europé 1375–1989. Tectonophysics 207, 1–23.

Andersen O B, Kejlsö E & Remmer O 1974. Secular movements within Jutland as determined from repeated precise levellings. Geodaet. Inst. Skr. 3. rk. 40. 1–70.

Andersen S, Erikstad L, Ingólfsson Ó, Lundqvist J, Pedersen S S, Salonen V-P, Selonen O & Vilborg L 1998. Israndlinier i Norden. TemaNord Miljö. Nordisk Ministerråd.

Andrews J T 1970. A Geomorphological Study of Post-Glacial Uplift, with Particular Reference to Arctic Canada: Institute of British Geographers. Special Publication No. 2, 1–156.

Ansorge J, Blundell D & Mueller St 1992. Europés lithoshere – seismic structure. In A continent revealed. The European Geotraverse. Ed. D. Blundell, R. Freeman & St. Mueller, 33–69.

Anundsen K 1985. Changes in shore-level and ice-front position in Late Weichselian and Holocene, southern Norway. Norsk Geografisk Tidskrift 39, 205–225.

Asklund B 1935. Gästrikländska fornstrandlinjer och nivåförändringsproblemen. Sveriges Geologiska Undersökning C 391, 1–119.

Bakkelid S 1979. Et forelöpig totalbilde av landhevningen i Norge. Norges Geografiske Oppmålning, 1– 22.

Bennike O & Jensen J B 1995. Near-shore Baltic Ice Lake deposits in Fakse Bugt, southeast Denmark. Boreas 24, 185–195.

Berglund B 1966. Late-Quaternary vegetation in eastern Blekinge, southeastern Sweden. A pollen-analytical study. I. Late-Glacial time. Opera Botanica, 12. 1–180.

Berglund M 1995. The Late Weichselian deglaciation, vegetational development and shore displacement in Halland, southwestern Sweden. University of Lund, Department of Quaternary Geology, Thesis 35, 1–113.

Bird E C F & Klemsdal T 1986. Shore displacement and the origin of the lagoon at Brusand, southwestern Norway. Norsk Geografisk Tidskrift 40, 27–35.

Björck S 1979. Late Weichselian stratigraphy of Blekinge, SE Sweden, and water level changes in the Baltic Ice Lake. University of Lund, Department of Quaternary Geology, Thesis 7, 1–248.

Björck S & Digerfeld G 1982. Late Weichselian shore displacement at Hunneberg, southern Sweden, indicating complex uplift. Geologiska Föreningens i Stockholm Förhandlingar 104, 132–155.

Björck S & Digerfeld G 1991. Alleröd-Younger Dryas sea level changes in south-western Sweden and their relation to the Baltic Ice Lake development. Boreas 20, 115–133.

Björck S 1995. A reviw of the history of the Baltic Sea, 13.0–8.0 ka BP. Quaternary International 27, 19–40.

Brunnberg L, Miller U & Risberg J 1985. Project Eastern Svealand: Development of the Holocene landscape. ISKOS 5, 85–91.

Caldenius C & Linman G 1949. En senkvartär regressions- och transgressionslager-följd vid Halmstad. Sveriges Geologiska Undersökning C 502, 1–26.

Caldenius C, Larsson W, Mohrén E, Linman G & Tullström H 1966. Beskrivning till kartbladet Halmstad. Sveriges Geologiska Undersökning Aa 198, 1–138.

Cathles L M 1975. The viscosity of the earth's mantle. Princeton University Press, Princeton, New Jersey,1–386.

Cato I 1992. Shore displacement data based on lake isolations confirm the postglacial part of the Swedish Geochronological Time Scale. Sveriges Geologiska Undersökning Ca 81, 75–80.

Christensen C 1993. Land and sea. In: Hvass & Stovgaard (eds). Digging into the past – 25 years of Archaeology in Denmark. Aarhus Universitetsforlag, 20–23.

Clark R D, Farrell W E & Peltier W R 1978. Global changes in postglacial sea level: a numerical calculation. Quaternary Research 9: 265–278.

Danielsen A 1970. Pollen-analytical Late-Quaternary studies in the Ra district of Östfold, southeast Norway. Årsbog for universitetet i Bergen, mat.-naturv. serie 1969:14, 1–143.

De Geer G 1888 (1890). Om Skandinaviens nivåförändringar under qvartärperioden. Sveriges Geologiska Undersökning C 161, 1–160.

Digerfeldt G 1975. A standard profile for Littorina transgression in western Skåne, South Sweden. Boreas 4, 125–142.

Dolukhanov P M 1979. The Quaternary History of the Baltic. Leningrad and Soviet Carelia. In: V Gudelis & L-K Königsson (eds), The Quaternary History of the Baltic, 115–125. Acta Universitatis Upsaliensis Symposia Univesitatis Upsaliensis Annum Quingentesimum Celebrantes 1. Uppsala.

Donner J 1980. The determination and dating of synchronous Late Quaternary shore-lines in Fennoscandia. In: N.A. Mörner (Ed.), Earth Rheology, Isostasy and Eustasy. Wiley, New York; N.Y, 285–293.

Ekman M 1986. A reinvestigation of the world's second longest series of sea level observations: Stockholm 1774–1984. National Land Survey of Sweden, Professional Papers 1986:4.

Ekman M 1996. A Consistent Map of the Postglacial Uplift of Fennoscandia. Terra Nova 8, 158–165.

Ekman M & Mäkinen J 1996. Recent postglacial rebound, gravity change and mantle flow in Fennoscandia. Geophysical Journal International 126, 229–234.

Emery K O & Aubrey D G 1991. Sea levels, land levels, and tide gauges. Springer-Verlag, 1–237.

Eronen M 1976. A radiocarbon-dated Ancylus transgression site in south-eastern Finland. Boreas 5, 65–76.

Eronen M & Haila H 1982. Shorelines displacement near Helsinki, southern Finland, during the Ancylus Lake stage. Annales Academiae Scientiarum Fennicae AIII 134, 111–129.

Eronen M 1983. Late Weichselian and Holocene shore displacement in Finland. In D.E. Smith & G. Dawson (eds.): Shorelines and Isostacy. Institute of British Geographers, Special Publication 16, Academic Press, 1983, 183–207.

Eronen M, Glückert G, van de Plassche O, van der Plicht J & Rantala P 1995. Land uplift in the Olkiluoto-Pyhäjärvi area, southwestern Finland, during the last 8 000 years. Nuclear Waste Commission of Finnish Power Companies, Report YJT-95-17, 1–26.

Fairbanks R G 1989. A 17 000-years glacio-eustatic sea level record: influence of glacial melting rates on the Younger Dryas event and deep-ocean circulation. Nature 342, 637–642.

Fairbridge R W 1961. Eustatic changes in sea level. Physics and Chemistry of the Earth 4, 99–185.

Fjeldskaar W & Cathles L 1991. Rheology of mantle and lithosphere inferred from post-glacial uplift in Fennoscandia. In: Sabdini et al. (eds): Glacial isostasy, sea-level and mantle rheology, Kluwer Academic Publishers, 1–19.

Fjeldskaar W 2000. How important are elastic deflections in the Fennoscandian postglacial uplift? Norsk Geologisk Tidskrift 80, 57–62.

Gembert B 1987. Sedimentological studies of a beach ridge system in Ottenby, Öland, South-eastern Sweden and related sea level changes in the Baltic basin. Striae 27, 1–66.

Glückert G 1976. Post-glacial shore-level displacement of the Baltic in SW Finland. Annales Academiae Scientiarum Fennicae AIII 134, 1–92.

Glückert G 1978. Östersjöns postglaciala strandförskjutning och skogens historia på Åland. Publication Department of Quaternary Geology, University of Turku, 1–106.

Glückert G & Ristaniemi O 1982. The Ancylus transgression west of Helsinki, South Finland – A preliminary report. Annales Academiae Scientiarum Fennicae AIII 134, 99–134.

Godwin H, Suggate R P & Willis E H 1958. Radiocarbon dating of the eustatic rise in ocean-level. Nature 181, 1518–1519.

Hafsten U 1983. Shore-level changes in South Norway during the last 13,000 years, traced by biostratigraphical methods and radiometric datings. Norsk Geografisk Tidskrift 37, 63–79.

Hald M & Vorren T O 1983. A shore displacement curve from the Tromsö district, North Norway. Norsk Geologisk Tidskrift 63, 103–110.

Hedenström A & Risberg J 1999. Early Holocene shore-displacement in southern central Sweden as recorded in elevated isolated basins. Boreas 28, 490–504.

Helle SK, Anundsen K, Aasheim S & Hafildason H 1997. Indications of a younger Dryas marine transgression in inner Hardanger, West Norway. Norsk Geologisk Tidskrift 77, 101–117.

Henningsmoen K E 1979. En karbon-datert strandforskyvningskurve fra söndre Vestfold. 239–247. In. Nydal, R, Westin, S, Hafsten, U & Gulliksen, S: Fortiden i sökelyset. Trondheim. (Univ. forl.)

Hyvärinen H 1980. Relative sea-level changes near Helsinki, southern Finland during early Litorina times. Bullentin of the Geological Society of Finland 52, 207–219.

Hyvärinen H 1984. The Mastogloia stage in the Baltic Sea history: Diatom evidence from southern Finland. Bullentin of the Geological Society of Finland 56. 1–2, 99–115.

Jelgersma S 1961. Holocene sea level changes in the Netherlands. Meded. Geol. Sticht., C, VI, 7. 1–100.

Jensen J B, Bennike O, Witkowski A, Lemke W & Kuijpers A 1999. Early Holocene history of the southwestern Baltic Sea: the Ancylus Lake stage. Boreas 28, 437–453.

Kabailiené M 1997. Shore line displacement, palaeoecological conditions and human impact on the southeastern coast of Baltic sea. In: The fifth marine geological conference "The Baltic", A Gregelis (ed.), 114–122. Lihuanian Institute of Geology. Vilinius 1997.

Kakkuri J 1987. Character of the Fennoscandian land uplift in the 20th century. Geological Survey of Finland, Special Paper 2, 15–20.

Kaland P E 1984. Holocene shore displacement and shorelines in Hordaland, western Norway. Boreas 13, 203–242.

Kaland P E, Krzywinski, K & Stabell B 1984. Radiocarbondating of the transitions between marine and lacustrine sediments and their relation to the development of lakes. Boreas 13, 243–258.

Kessel H & Raukas A 1979. The Quaternary History of the Baltic, Estonia. In: V Gudelis & L-K Königsson (eds), The Quaternary History of the Baltic, 127–146. Acta Universitatis Upsaliensis Symposia Universitatis Upsaliensis Annum Quingentesimum Celebrantes 1. Uppsala.

Kjemperud A 1986. Late Weichselian and Holocene shore displacement in the Trondheimsfjord area, central Norway. Bores 15, 61–82.

Klug H 1980. Der Anstieg des Ostseespiegels im deutchen Küstenraum set dem Mittelatlantikum. Eiszeitalter und Gegenwart 30, 237–252.

Krzywinski K & Stabell B 1984. Late Weichselian sea level changes at Sotra, Hordaland, western Norway. Boreas 13, 159–202.

Kääriäinen E 1963. Land uplift in Finland computed by aid of precise levellings. Fennia 89, 15–19.

Kääriäinen E 1966. The second levelling of Finland in 1935–1955. Veröff. Finn. Geodät. Inst. 61, Helsinki, 1–331.

Lagerbäck R 1988. Postglacial faulting and paleoseismicity in the Lansjärv area, northern Sweden. SKB TR 88-25, 1–37, Svensk Kärnbränslehantering AB.

Lagerbäck R 1990. Late Quaternary faulting and paleoseismicity with particular reference to the Lansjärv area, northern Sweden. Geologiska Föreningens i Stockholm Förhandlingar 112, 333–354.

Lambeck K 1991. A model for Devensian and Flandrian glacial rebound and sea-level change in Scotland. In: Sabdini et al. (eds): Glacial isostasy, sea-level and mantle rheology, Kluwer Academic Publishers, 33–61.

Lambeck K, Smither C & Johnston P 1998. Sea-level change, glacial rebound and mantle viscosity for northern Europe. Geophysical Journal International 134, 102–144.

Liljegren R 1982. Paleoekologi och strandförskjutning i en Littorinavik vid Spjälkö i mellersta Blekinge. University of Lund, Department of Quaternary Geology, Thesis 11, 1–95.

Lisitzin E 1974. Sea-level changes. Elsevier Scientific Publishing Co. 1974.

Lundqvist G 1962. Geological radiocarbon datings from the Stockholm station. Sveriges Geologiska Undersökning C 589, 1–23.

McConnell R K 1968. Viscosity of the Mantle from Relaxation Time Spectra of Isostatic Adjustment: J. Geophys. Res.73, 7089–7105.

Miller U & Robertsson A-M 1982. The Helgeandsholmen excavation: An outline of biostratigraphical studies to document shore displacement and vegetational changes. PACT 7, 311–327.

Miller U & Robertsson A-M 1988. Late Weichselian and Holocene environmental changes in Bohuslän, Southwestern Sweden. Geographia Polonica 55, 103–111.

Morén L & Påsse T 2001. Climate and shoreline in Sweden during Weichsel and the next 150 000 years. SKB TR in progress.

Möller J J 1984. Holocene shore displacement at Nappstraumen, Lofoten, North Norway. Norsk Geologisk Tidskrift 64, 1–5.

Mörner N A 1969. The Late Quaternary History of the Kattegatt Sea and the Swedish West Coast. Sveriges Geologiska Undersökning C 640, 1–487.

Mörner N A 1976. Eustatic changes during the last 8,000 years in view of radiocarbon calibration and new information from the Kattegatt region and other northwestern European coastal areas. Palaeogeography, Palaeoclimatology, Palaeoecology, 19, 63–85.

Mörner N A 1980. The Northwest European "sea-level laboratory" and regional Holocene eustasy. Palaeogeography, Palaeoclimatology, Palaeoecology, 29, 281–300.

Nakada M & Lambeck K 1987. Glacial rebound and relative sea-level variations: a new appraisal. Geophysical Journal Royal Astronomical Society 90, 171–224.

Nakada M & Lambeck K 1989. Late Pleistocene and Holocene sea-level change in the Austrailian region and mantle rheology. Geophysical Journal 96. 497–517.

Nakiboglu S M & Lambeck K 1991. Secular sea-level change. In: Sabdini et al. (eds): Glacial isostasy, sea-level and mantle rheology, Kluwer Academic Publishers, 237–258.

Nilsson E 1968. Södra Sveriges senkvartära historia. Geokronologi, issjöar och landhöjning. Kungliga Svenska Vetenskapsakademiens Handlingar. Fjärde serien. Band 12. Nr 1, 1–117.

Peltier W R 1976. Glacial isostatic adjustments – II: The inverse problem. Geophysical Journal Royal Astronomical Society 46, 605–646.

Peltier W R 1988. Lithospheric thickness, Antarctic deglaciation history, and ocean basin discretization effect in a global model of postglacial sea level changes: a summary of some sources of nonuniqueness. Quaternart Reaserch 29. 93–112.

Peltier W R 1991. The ICE-3G model of late Pleistocene deglaciation: construction, verification, and applications. In: R. Sabadini et al. (Editors), Glacial,Isostasy, Sea-level and Mantle Rheology. Kluwer, Dordrecht, 95–119.

Persson G 1962. En transgressionslagerföljd från Limhamn. Geologiska Föreningens i Stockholm Förhandlingar 84, 47–55.

Persson G 1973. Postglacial transgressions in Bohuslän, Southwestern Sweden. Sveriges Geologiska Undersökning C 684, 1–47.

Persson C 1979. Shore displacement during Ancylus time in the Rejmyra area, south central Sweden. Sveriges Geologiska Undersökning C 755, 1–23.

Påsse T 1983. Havsstrandens nivåförändringar i norra Halland under Holocen tid. Göteborgs universitet. Geologiska institutionen A 45,1–174.

Påsse T 1986. Beskrivning till jordartskartan Kungsbacka SO. Sveriges Geologiska Undersökning Ae 56, 1–106.

Påsse T 1987. Shore displacement during the Late Weichselian and Holocene in the Sandsjöbacka area, SW Sweden. Geologiska Föreningens i Stockholm Förhandlingar 109, 197–210.

Påsse T 1988. Beskrivning till jordartskartan Varberg SO/Ullared SV. Sveriges Geologiska Undersökning Ae 86, 1–98.

Påsse T 1990a. Emperical estimation of isostatic uplift using the lake-tilting method at Lake Fegen and at Lake Säven, southwestern Sweden. Mathematical Geology 22, No. 7, 803–824.

Påsse T 1990b. Beskrivning till jordartskartan Varberg NO. Sveriges Geologiska Undersökning Ae 102, 1–117.

Påsse T 1996a. Lake-tilting investigations in southern Sweden. SKB TR 96-10, 1–34, Svensk Kärnbränslehantering AB.

Påsse T 1996b. A mathematical model of the shore level displacement in Fennoscandia. SKB TR 96-24, 1–92, Svensk Kärnbränslehantering AB.

Påsse T 1997. A mathematical model of past, present and future shore level displacement in Fennoscandia. SKB TR 97-28, 1–55, Svensk Kärnbränslehantering AB.

Påsse T 1998. Lake-tilting, a method for estimation of isostatic uplift. Boreas 27. 69–80.

Påsse T & Andersson L 2000. A mathematical shore level model presented in GIS. Geologiska Vintermötet i Trondheim. Abstract.

RAK (Rikets allmänna kartverk) 1971. Geodetic activities in Sweden 1967–1970. Geographical Survey Office of Sweden A 38, 1–19.

RAK (Rikets allmänna kartverk) 1974. Sveriges andra precisionsavvägning 1951–1967. Geographical Survey Office of Sweden A 40, 1–91.

Ramfjord H 1982. On the Late Weichselian and Flandrian shoreline displacement in Naeröy, Nord-Tröndelag, Norway. Norsk Geologisk Tidskrift 62, 191–205.

Renberg I & Segerström U 1981. The initial points on a shoreline displacement curve for southern Västerbotten, dated by varve-counts of lake sediments. Striae 14, 174–176.

Richardt N 1996. Sedimentological examination of the Late Weichselian sea-level history following deglaciation of northern Denmark. Geological Society Special Publication 111, 261–273.

Ringberg B 1989. Upper Late Weichselian lithostratigraphy in western Skåne, southernmost Sweden. Geologiska Föreningens i Stockholm Förhandlingar 111, 319–337.

Risberg J 1991. Palaeoenvironment and sea level changes during the early Holocene on the Södertörn penisula, Södermanland, eastern Sweden. Stockholm University, Department of Quaternary Research. Report 20, 1–27.

Robertsson A-M 1991. Strandförskjutningen i Eskiltunatrakten för ca 9 000 till 4 000 år sedan. Sveriges Geologiska Undersökning, Rapporter och meddelanden 67, 1–27.

Robertsson A-M 1997. Shore displacement in north-eastern Småland c. 9 000–2 500 BP. In Cato & Klingberg (eds.): Proceedings of the Fourth Marine Geological Conference – the Baltic, Uppsala 1995. Sveriges Geologiska Undersökning Ca 86, 145–152.

Saarnisto M 1981. Holocene emergence history and stratigraphy in the area north of the Gulf of Bothnia. Annales Academiae Scientiarum Fennicae AIII 130, 1–42.

Salomaa R 1982. Post-glacial shoreline displacement in the Lauhanvuori area, western Finland. Annales Academiae Scientiarum Fennicae AIII 134, 81–97.

Salomaa R & Matiskainen H 1983. Rannan siirtyminen ja arkeologinen kronologia Etelä-Pohjanmaalla. Arkeologian päivät 7–8.4.1983 Lammin Biolog. tutkimusasemalla. Karhunhammas 7, 21–36.

Salonen V-P, Räsenen M & Terho A 1984. Palaeolimnology of ancient Lake Mätäjärvi. Third Nordic Conference on the application of scientific methods in archaelogy. Mariehamn, Åland, Finland, 8–11 October 1984. Iskos 5, 233–288.

Sauramo M 1944. Landhöjningens mekanism. Geologiska Föreningens i Stockholm Förhandlingar 66, 536–550.

Shepard F P 1963. Submarine Geology. Harper and Row, New York, N.Y. 2nd ed., 1–557.

Simonsen O 1969. Some remarks in May 1968 on the secular movements within Denmark. In. J A Mescherikov, Problems of recent crustal movements of the Earth, USSR Acad. Sci., Moscow.

Snyder J A, Korsun S A & Forman S L 1996. Postglacial emergence and Tapes transgression, north-central Kola Penisula, Russia. Boreas, 47–56.

Solem T & Solem J O 1997. Shoreline displacement on the coast of Sör-Tröndelag and Möre og Romsdal, Central Norway; a botanical and zoological approach. Norsk Geologisk Tidskrift 77, 193–203.

Stabell B 1980. Holocene shorelevel displacement in Telemark, southern Norway. Norsk Geoglogisk Tidskrift 60, 71–81.

Suutarinen O 1983. Recomputation of land uplift values in Finland. Reports of the Finnish Geodetic Institute 83:1, 1–16.

Svedhage K 1985. Shore displacement during Late Weichselian and Early Holocene in the Risveden area, SW Sweden. Göteborgs universitet. Geologiska institutionen A 51, 1–111.

Sveian H & Olsen L 1984. En strandforsyvningskurve fra Verdalsöra, Nord-Tröndelag. Norsk Geologisk Tidskrift 64, 27–38.

Svendsen J I & Mangerud J 1990. Sea-level changes and pollen stratigraphy on the outer coast of Sunnmöre, western Norway. Norsk Geologisk Tidskrift 70, 111–134.

Svensson N-O 1989. Late Weichselian and Early Holocene shore displacement in the Central Baltic, based on stratigraphical and morphological records from Eastern Småland and Gotland, Sweden. Lund University, Department of Quaternary Geology 25, 1–195.

Sörensen R 1979. Late Weichselian deglaciation in the Oslofjord area, south Norway. Boreas 8, 241–246.

Thomsen H 1981. Late Weichselian shore-level displacement on Nord-Jären, south-west Norway. Geologiska Föreningens i Stockholm Förhandlingar 103, 447–468.

Tirén S, Beckholmen M & Isaksson H 1987. Structural analysis of digital terrain models, Simpevarp area, south-eastern Sweden. SKB PR 25-87-21, 1–51, Svensk Kärnbränslehantering AB.

Tirén S & Beckholmen M 1988. Structural analysis of the Simpevarp area, south-eastern Sweden, Lineaments and rock blocks. SKB PR 25-88-01, 1–57, Svensk Kärnbränslehantering AB.

Winn K, Averdieck F R, Erlenkeusser H & Werner F 1986. Holocene sea level rise in western Baltic and the question of isostatic subsidence. Meyniana 38, 61–80

Vorren K-D & Moe D 1986. The early Holocene climate and sea-level changes in Lofoten and Vesterålen, North Norway. Norsk Geologisk Tidskrift 66, 135–143.

Vorren T, Vorren K-D, Alm T, Gulliksen S & Lövlie R 1988. The last deglaciation (20,000 to 11,000 B.P.) on Andöya, northern Norway. Boreas 17, 41–77.

Åse L-E 1970. Kvartärbiologiska vittnesbörd om strandförskjutningen vid Stockholm under de senaste c. 4000 åren. Geologiska Föreningens i Stockholm Förhandlingar 92, 49–78.